 Open File 80-466

UNITED STATES
DEPARTMENT OF THE INTERIOR
GEOLOGICAL SURVEY

Mail Stop 964, Federal Center, Box 25046
Denver, Colorado 80225

Resistivity sounding investigation by the Schlumberger method in the Syncline Ridge area, Nevada Test Site, Nevada

Prepared by the U.S. Geological Survey

for

Nevada Operations Office
U.S. Department of Energy
(Memorandum of Understanding EW-78-A-08-1543)

Open File 80-466 Open File 80-466

UNITED STATES
DEPARTMENT OF THE INTERIOR
GEOLOGICAL SURVEY

Mail Stop 964, Federal Center, Box 25046
Denver, Colorado 80225

Resistivity sounding investigation by the Schlumberger method in the Syncline Ridge area, Nevada Test Site, Nevada

by

L. A. Anderson, R. J. Bisdorf, and D. R. Schoenthaler

Open-File Report 80-466

1980

This report is preliminary and had not been
edited or reviewed for conformity with U.S.
Geological Survey standards.

Prepared by the U.S. Geological Survey

for

Nevada Operations Office
U.S. Department of Energy
(Memorandum of Understanding EW-78-A-08-1543)

Resistivity sounding investigation by the Schlumberger method in the Syncline Ridge area, Nevada Test Site, Nevada

by

L. A. Anderson, R. J. Bisdorf, and D. R. Schoenthaler

Introduction

A resistivity survey was made in the north-central sector of the Nevada Test Site (NTS) as part of an extensive search for suitable geologic environments to be used as repositories for radioactive waste products. The area of interest, identified herein as Syncline Ridge after a locally prominent structural feature, lies within the Tippipah Spring Quadrangle, part of which is shown in figure 1. Figure 1 includes the surficial geology generalized from Orkild (1963), mapped and inferred faults, resistivity sounding sites, borehole emplacements, and alinements of resistivity cross sections compiled from the interpreted sounding data. The intent of the survey was to determine the horizontal continuity and thickness of unit J of the Eleana Formation. Ten distinct lithologic units make up the Eleana Formation but only units G, H, I, and J of Mississippian age are found in the Syncline Ridge area. Because of its relative importance in this survey, unit J is shown in figure 1 as a separate entity, whereas the G, H, and I units have been grouped under the general heading of Eleana Formation.

Unit J is primarily an argillaceous argillite containing interbedded layers of quartzite, limestone, and siliceous sandstone (Orkild, 1963). The argillaceous sections of the argillite are considered to be especially suitable as a containment media for radioactive waste material because of the fine-grained nature of the contained clay minerals. The clays provide for an extremely low fluid permeability and add a plastic quality to the argillite such that a high degree of stress can be absorbed before rock rupture occurs.

The clay in the argillite also serves to reduce the electrical resistivity of the rock through surface conductance and ion exchange processes (Keller and Frischknecht, 1966) imparting an electrical property to the argillite which allows it to be distinguished from other rock types.

To demonstrate resistivity variations with rock type, a digitized resistivity log from borehole UE16F (fig. 1) is shown correlated with the lithology of the penetrated section in figure 2A. The resistivity log was digitized from electric logs, obtained with a 64-inch normal electrode array, by Douglas Muller of the U.S. Geological Survey. The borehole is entirely within unit J of the Eleana Formation and, with the exception of the 15-meter sandstone section near the top of the drill hole, the rock types are either argillite or quartzite and, conceivably, mixtures of the two. The thickest section of argillite is located at the 160-295 meter depth interval having an average resistivity value of about 20 ohm-m. Those layers identified as quartzite may have resistivities as high as 300 ohm-m depending upon the argillite/quartzite ratio. Presumably the low resistivity parts of the log within the 295-300 meter interval identified as quartzite represent virtually all argillite. The 15 meter thick sandstone layer underlying the alluvium approaches a resistivity of 70 ohm-m.

A similar comparison between resistivity and lithology using data from borehole UE16d (fig. 1) is shown in figure 2B. The 25 to 453 meter interval is Tippipah Limestone having a resistivity generally in excess of 1,000 ohm-m. Thrust faults separate the upper 90 meter section of unit J of the Eleana Formation from the lower Eleana and the overlying Tippipah Limestone. This section contains a substantial quantity of limestone accounting for the high resistivities observed within this interval. Below the 542 meter level the prevalent rock types are quartzite and argillite, however, the high resistivity zones within the 542 and 625 depth interval are probably caused by competent layers of limestone. Where argillite is predominant resistivities rarely exceed 40 ohm-m. At depths between 755-790 meters quartzite is most abundant resulting in resistivities in excess of 100 ohm-m.

Using the resistivity/rock relationship inferred from the borehole logs as a guide to identifying that which is argillite, vertical electrical soundings were made near Syncline Ridge and in an area to the north, east of the Eleana Range. A total of 44 soundings were made. The field data were interpreted in terms of rock layer resistivity and thickness by computer methods and cross-sections were constructed to demonstrate lateral resistivity variations within the near-surface rock.

Vertical electrical soundings

Resistivity soundings were made with a four electrode configuration commonly referred to as the Schlumberger array (Keller and Frischknecht, 1966). The method uses four in-line electrodes; the inner pair for recording electrical potential as a current is passed through the outer pair. Measurements are made using direct current for a series of readings involving successively larger current electrode separations. The data are plotted on a logarithmic scale to produce a sounding curve representing vertical resistivity variations centered about the midpoint of the array. The greater the distance between current and potential electrodes the greater the depth of exploration. Sounding curves 1 to 44 (appendix A) show the results of those measurements made at the locations indicated in figure 1. The soundings are numbered in the sequence in which they were obtained. Each sounding curve is accompanied by an interpretation in the form of a geoelectric section obtained through an updated version of a computer method developed by Adel Zohdy of the U.S.G.S. (Zohdy, 1974a, 1975).

Sounding results

Soundings 1 through 44 (appendix 1) each show the measured field data as diamonds connected by straight line segments; the squares portray a shifted field curve obtained by vertical adjustment of individual segments relative to that segment on the right-hand side of the sounding curve (Zohdy and others, 1973); and the plus symbols are theoretical data points obtained for the indicated geoelectric section as interpreted from the shifted field data. The geoelectric section is represented by the columnar graph wherein the width of a particular column designates the thickness of an individual layer and its vertical position corresponds to the resistivity of that layer. The dotted profile is the corresponding Dar Zarrouk curve (DZ) (Zohdy, 1974b) for the interpreted geoelectric section which can be used to further refine the geoelectric section by reducing the layering to a fewer number of equivalent layers.

Interpretation of the sounding data assumes homogeneous, horizontal layering, therefore, where lateral heterogeneities in resistivity exist within the influence of the energizing current field, the sounding curve may exhibit distortions which, when present, the computer will attempt to interpret as layering. Data distortion resulting from lateral variations in rock resistivity are not always recognizable from the shape of the field curve but these effects become obvious when soundings sharing a common midpoint are expanded such that the individual electrode alinements are mutually perpendicular. As an example, soundings 6 and 15 centered at the same locations and expanded along those azimuths shown in figure 1 demonstrate differences attributed to horizontal variations in rock type. The soundings are essentially the same out to a spacing (AB/2) of 25 meters. At greater electrode spacings, sounding 6 becomes somewhat irregular in appearance whereas sounding 15 remains smooth and generally flat. The differences are ascribed to the probability that sounding 6 was expanded perpendicular to some lateral structure while sounding 15 parallelled the structure. This is counter to what may be inferred from the surface geology and drainage directions. However, the wide differences in the interpreted geoelectric section of sounding 6 as compared to that of sounding 23, the latter located approximately 740 meters south of sounding site 6, strongly suggests the existence of an east-west trending fault within that interval between sounding locations. If the inferred fault represents a lateral resistivity change the distortive effect would be most notable on sounding 6 as the current electodes are expanded over and beyond the fault trace. Conversely, an array expanded parallel to an offset structure would tend to average the resistivity of the total rock volume penetrated by the flow of current.

For an unbiased automatic computer interpretation, the resistivity assigned to the lowermost layer depends in part on the data point taken at the largest electrode separation. On sounding 15 there is a slight increase in the resistivity of the last data point relative to the preceding point, therefore the bottom layer, extrapolated to depth, is interpreted as having a high resistivity. The data points on sounding 6 at spacings greater than 1,000 meters indicate a trend towards a low bottom layer resisitivity and is interpreted accordingly. Actually the resistivity measured at the AB/2 electrode spacing of 1200 meters is virtually identical on both soundings. However, the foregoing as well as following data points on the sounding curve all act to influence the final selection of bottom layer resistivity as determined by the computer. Sounding 6 was fortunately expanded to an AB/2 spacing of 1830 meters which establishes a clearcut trend towards a relatively low resistivity for the deepest layer detected on the sounding curve.

Vertical geoelectric sections

Geoelectric cross sections were prepared from interpreted soundings to demonstrate resistivity variations within the various sectors of the study area. The sections were compiled with a 2:1 vertical exaggeration and contoured in geometric progression from a value of 20 ohm-m. Vertical scale is elevation above sea level in meters. In preparing a cross section, the data representing the uppermost 100 meters was generalized because of the wide range of resistivities measured in this interval. At many sounding locations the upper 100 meter section consists primarily of unconsolidated alluvial deposits varying from clay to gravel all of which may only be partially water saturated. Based on well data, the water table is reportedly about 130 meters from the surface in the northern part of the area and deepens to 225 meters in the southern part (J. E. Weir, oral communication, 1979).

Soundingsalong the eastern edge of Syncline Ridge and its northern extension were used to construct the resistivity cross section (A-A') shown in figure 3. The trend of the cross section is NNE to SSW (fig. 1). Southward from VES location 14 to VES 6 the resistivities are reasonably continuous and fairly high corresponding to a quartzite-limestone lithology. At sounding 10 the resistivities are sufficiently low to indicate the presence of argillite within the section. However, the close proximity of the sounding 10 location to several fault structures may have distorted the sounding curve resulting in an interpretation unrepresentative of the geoelectric section at that site.

As previously noted, a major discontinuity is evident between soundings 6 and 23. An apparent fault within this interval has caused an offset in lithology such that the southern part of the cross-section is of much lower resistivity. The resistivity is quite uniform in the upper section and is indicative of a quartzitic argillite corresponding to unit J of the Eleana Formation.

Figure 4 shows a cross section constructed from soundings made along Tippipah Spring and Back Mesa Roads (B-B', fig. 1). The cross section varies in direction but the trend is east-west transecting the grain of the principal structures in the region. The contoured data do not indicate lithologic uniformity across the section. As shown in figure 1, virtually every sounding on the cross section parallels a fault possibly causing a distortion of the sounding curve which is difficult to recognize in that particular sounding alinement relative to the fault direction. The resistivity variations within the section may therefore be somewhat attributable to lateral offsets affecting individual sounding measurements or by changes in lithology relating to any number of natural circumstances. In either case the resistivities are quite high probably representing quartzite and limestone. VES 18, in the central part of the valley situated between Syncline Ridge and the Eleana Range, shows evidence of argillaceous argillite (<40 ohm-m.) at depths greater than 400 meters.

A cross section (C-C', fig. 1) constructed from soundings alined with the major axis of the central valley is shown in figure 5. As before, data distortion owing to lateral effects may have caused an erroneous interpretation of the resistivity sounding data, particularly at VES sites 8 and 18 where the presence of faults are clearly indicated. At these locations there are discontinuities in the resistivity cross section which either reflect the position of the fault or are an indirect result of the fault through its effects on the shape of the sounding curve. Lateral effects are apparently diminished at the higher electrode spacings as evidenced by the fact that an unbroken layer of low resistivity rock extends at depth from VES 18 northward to VES 43. This low resistivity layer is identified with a thick section of argillaceous argillite. The resistivities in the southern part of the cross section in figure 5 are substantially higher indicating the likely presence of quartzite and limestone.

A cross section (D-D , fig. 1) parallel to that shown in figure 5 illustrates resistivity variations within the eastern part of the central valley between the Eleana Range and the northern extension of Syncline Ridge (fig. 6). Faults exist in close proximity to sounding sites 12 and 34 on the southern end accounting for the dramatic resistivity increase observed in that part of the cross section. North of VES 34 the resistivities are laterally continuous and sufficiently low within the near surface zone to be correlated with argillaceous argillite.

Figure 7 illustrates resistivity variations along an east-west cross section through the central part of the northern block (E-E', fig. 1). With the possible exception of VES site 24 on the eastern end of the cross section, there are no apparent faults to adversely affect the sounding curves. Low resistivities, attributable to argillaceous argillite, extend to an undetermined depth below sounding site 30 at the western end of the section. The implied argillite is continuous across the entire section but thins appreciably on the eastern end such that it exists only in the 200-300 meter interval in the vicinity of sounding 24. An interbed of what is possibly a more quartzitic variety of argillite is located within the western half of the cross section. This quartzitic member reaches a thickness in excess of 300 meters in the central part of the area.

Approximately 1.5 km north of cross section E-E' the cross section in figure 8 has been compiled from sounding data trending westerly from VES 40 to VES 22 and then northwest to VES 44 (F-F', fig. 1). A thick layer of low resistivity material equated with argillaceous argillite, occupies a major portion of the section. The inferred argillite thins to the west as the Eleana Range is approached and terminates abruptly near the eastern end somewhere between soundings 22 and 40. Low resistivities are detected at depth at sounding location 40 suggesting the probability of a vertical offset on the order of 900 meters having occurred along the west flank of the northern extension of Syncline Ridge.

To better illustrate the distribution of argillaceous argillite within the northern block, a fence diagram has been constructed connecting VES locations as shown in figure 9. The vertical lines drawn downward from the respective sounding sites signify the depth to which interpretation of layer resistivity was possible. The interconnecting hachured bands represent the distribution and thickness of rock having a resistivity of less than 40 ohm-meters. With the exception of sounding sites 34 and 40 a near surface layer persists throughout, generally at a depth of less than 100 meters and varying in thickness from 40 to 580 meters. A second and deeper layer of less tha 40 ohm-m, equated with argillaceous argillite, exists in the southern part of the block; the depth to the top varying from 245 to 660 meters. The bottom of this second layer was not detected except at VES sites 29 and 37; the thinnest section interpreted to be 220 m at sounding location 37. Although the lower layer does extend to the north as far as sounding 8 on the east flank of the Eleana Range, its horizontal extent is rather limited. The areal distribution of the deep layer is estimated to be not much greater than 2.25 sq. km.

Summary and Conclusions

The interpreted results of forty-four Schlumberger resistivity soundings made in the Syncline Ridge area within the Nevada Test Site indicate appreciable horizontal variations in lithology between the individual sounding locations. In part, this observation can be ascribed to variations within the rock type from one site to the other but, mostly the lateral resistivity changes are caused by structural offsets resulting from large-scale faulting of the rock formations. In either event the range of resistivities measured in most locations indicate the rocks to be characteristically high in quartz or limestone and therefore unsuitable as a storage media for nuclear waste products.

In the northern block of the central valley lying between the Eleana Range and the northern projection of Syncline Ridge a low resistivity member of the Eleana Formation, believed to consist primarily of argillaceous argillite, was found to be laterally continuous in the near surface environment. The layer is typically less than 150 meters thick except along the eastern side of the block where interpreted thicknesses are on the order of 300-600 meters. A much thicker low resistivity layer was detected in the southern part of the block at depths in excess of 250 meters. Although this lower layer has an appreciable thickness its horizontal extent is probably not sufficient to satisy the minimum requirements prescribed for potentially useable nuclear waste isolation sites.

In summarizing the results of the resistivity sounding surveys made in the general vicinity of Syncline Ridge and its northern extensions, it is apparent from the lithologic discontinuities observed in the constructed geoelectric cross-sections that the region has undergone a long history of tectonic upheaval. Based on this lack of structural integrity of the Eleana Formation and the limited extent of rock which can be identified as primarily argillaceous argillite, no suitable site can be clearly identified as having the necessary attributes for containing nuclear waste products.

References

Keller, George V., and Frischknecht, Frank C., 1966, Electrical methods in geophysical prospecting, Pergamon Press, London, New York, Toronto, 517 p.

Orkild, Paul P., 1963, Geologic map of the Tippipah Spring Quadrangle, Nye County, Nevada, U.S.G.S. Map GQ-213

Zohdy, A. A. R., Anderson, L. A., and Muffler, L. J. P., 1973, Resistivity, self potential, and induced polarization surveys of a vapor-dominated geothermal system: Geophysics, v. 38, no. 6, p. 1130-1144.

Zohdy, A. A. R., 1974a, A computer program for the automatic interpretation of Schlumberger sounding curves over horizontally layered media: NTIS (Natl. Tech. Inf. Service) PB-232 703/AS, 25 p., Springfield, Va.

_____1974b, The use of Dar Zarrouk curves in the interpretation of VES data: U.S. Geol. Survey Bull. 1313-D, 41 p.

_____1975, Automatic interpretation of Schlumberger sounding curves using modified Dar Zarrouk functions: U.S. Geol. Survey Bull. 1313-E, 39 p.

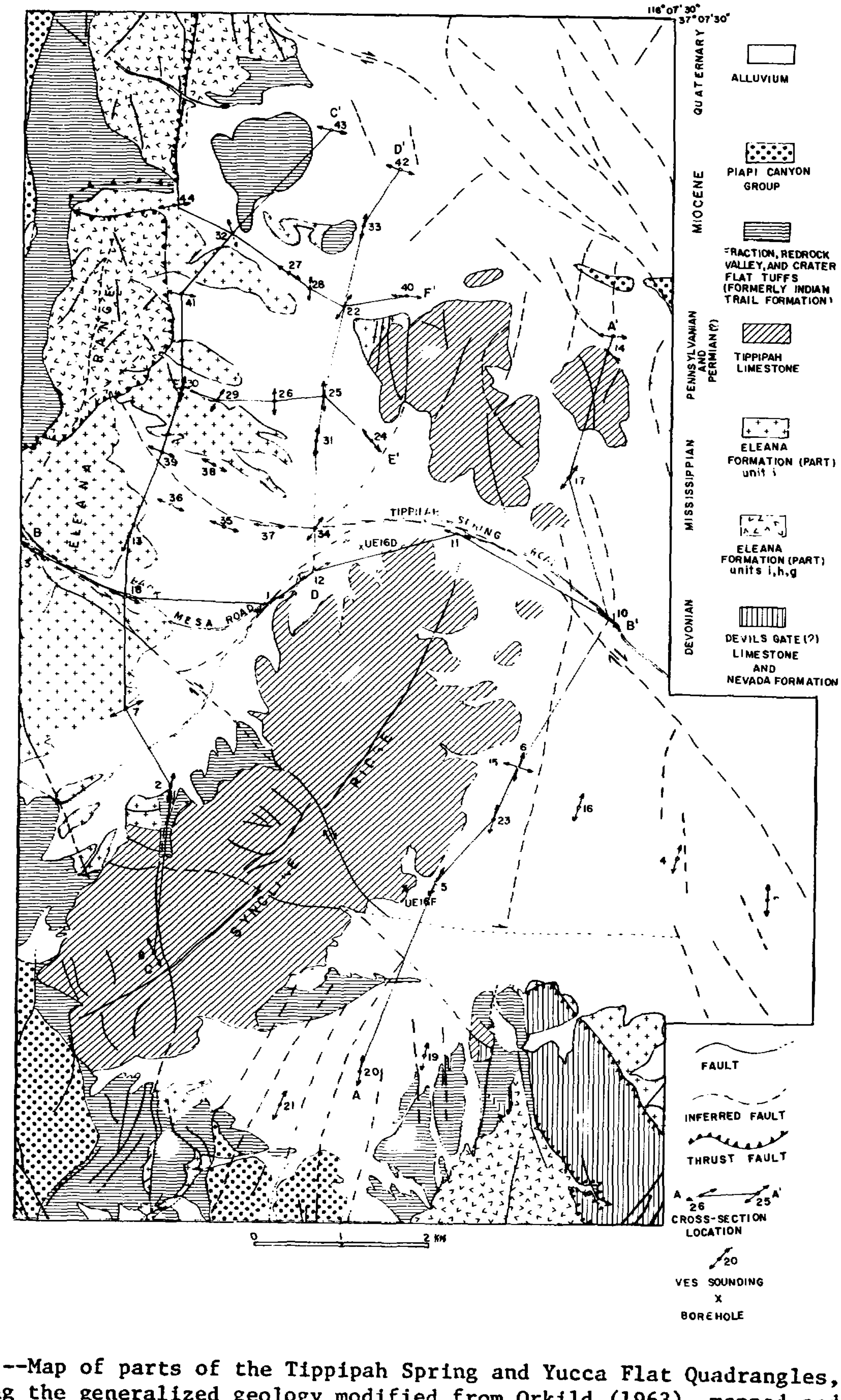

Figure 1.--Map of parts of the Tippipah Spring and Yucca Flat Quadrangles, Nev. showing the generalized geology modified from Orkild (1963), mapped and inferred faults, borehole and Schlumberger sounding locations, and the sounding alinement used in the compilation of geoelectric cross section.

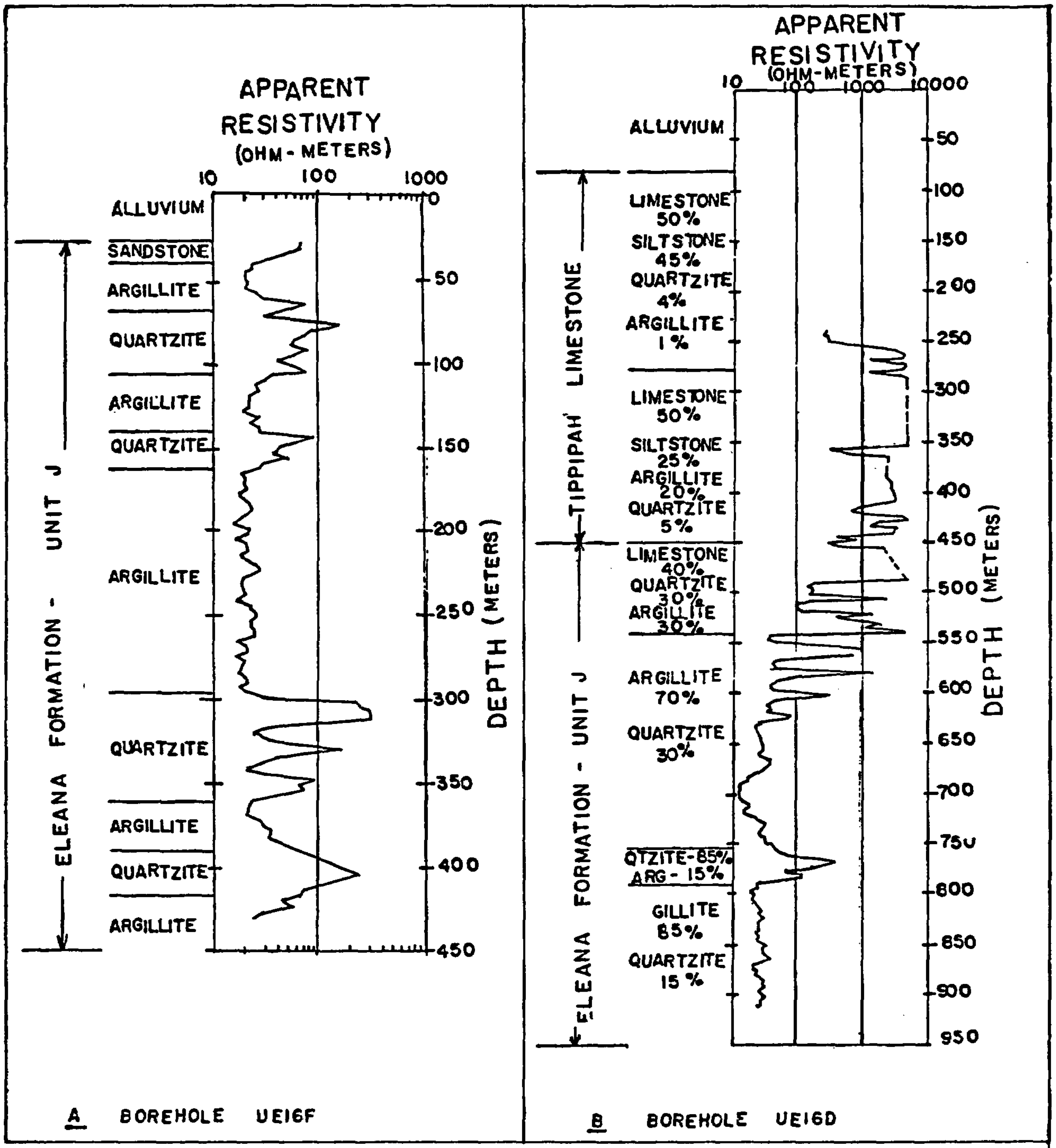

Figure 2.--Resistivity variations as a function of rock type determined from boreholes; A, UE16F; and B, UE16D located as shown in figure 1.

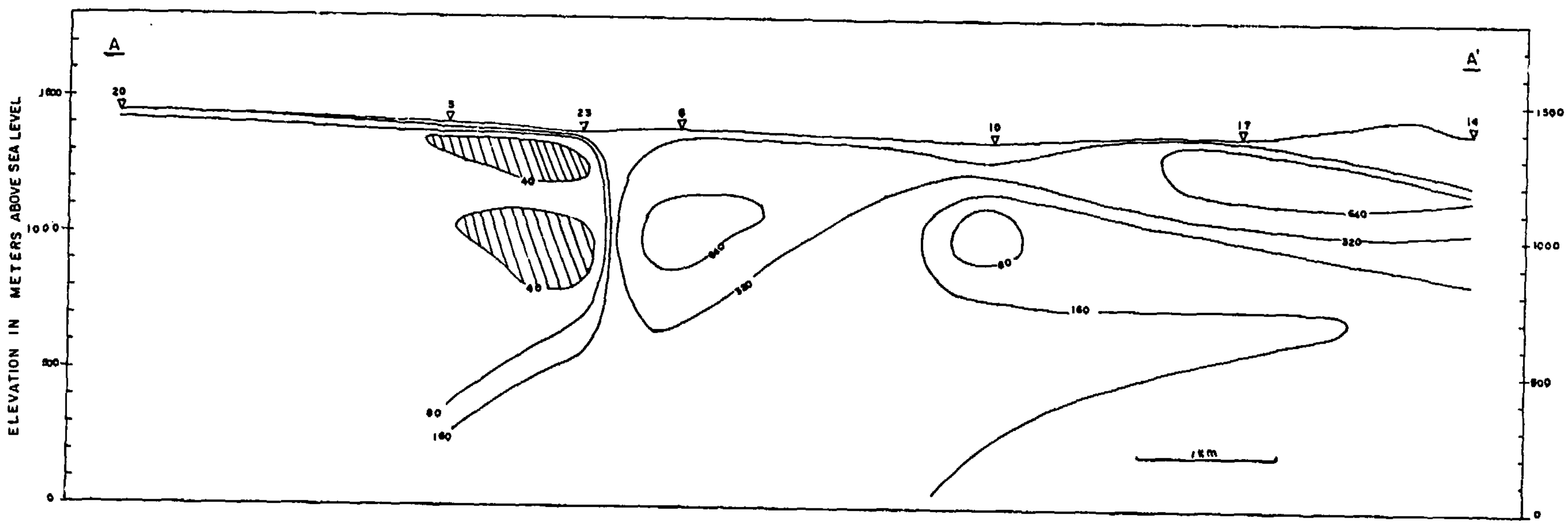

Figure 3.--Geoelectric cross-section A-A' (fig. 1) compiled from interpreted resistivity sounding data. Contours increase in geometric progression from a value of 20 ohm-meters. Patterned areas are those intervals considered to be composed primarily of argillaceous argillite of the Eleana Formation. Vertical exaggeration is 2X.

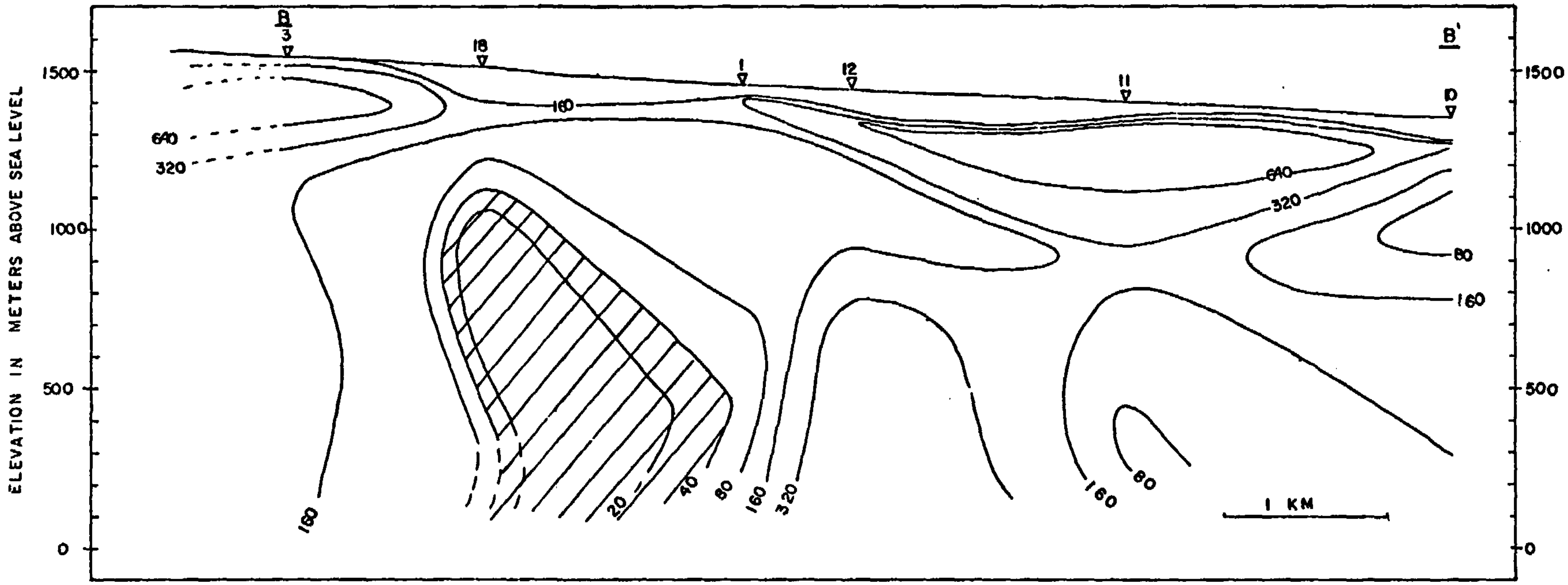

Figure 4.--Geoelectric cross-section B-B' (fig. 1) compiled from interpreted resistivity sounding data. Contours increase from a value of 20 ohm-meters. Dashed contours indicate inferred values of resistivity. Patterned areas are those intervals considered to be composed primarily of argillaceous argillite of the Eleana Formation. Vertical exaggeration is 2X.

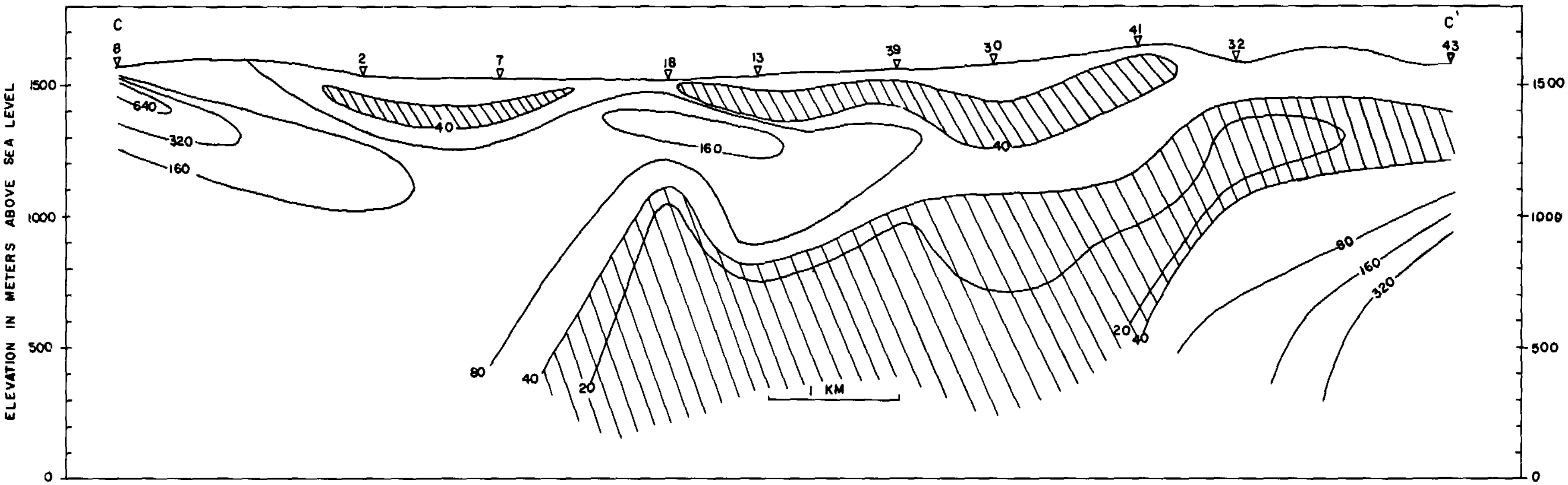

Figure 5.--Geoelectric cross-section C-C' (fig. 1) compiled from interpreted resistivity sounding data. Contours increase in geometric progression from a value of 20 ohm-meters. Patterned areas are those intervals considered to be composed primarily of argillaceous argillite of the Eleana Formation. Vertical exaggeration is 2X.

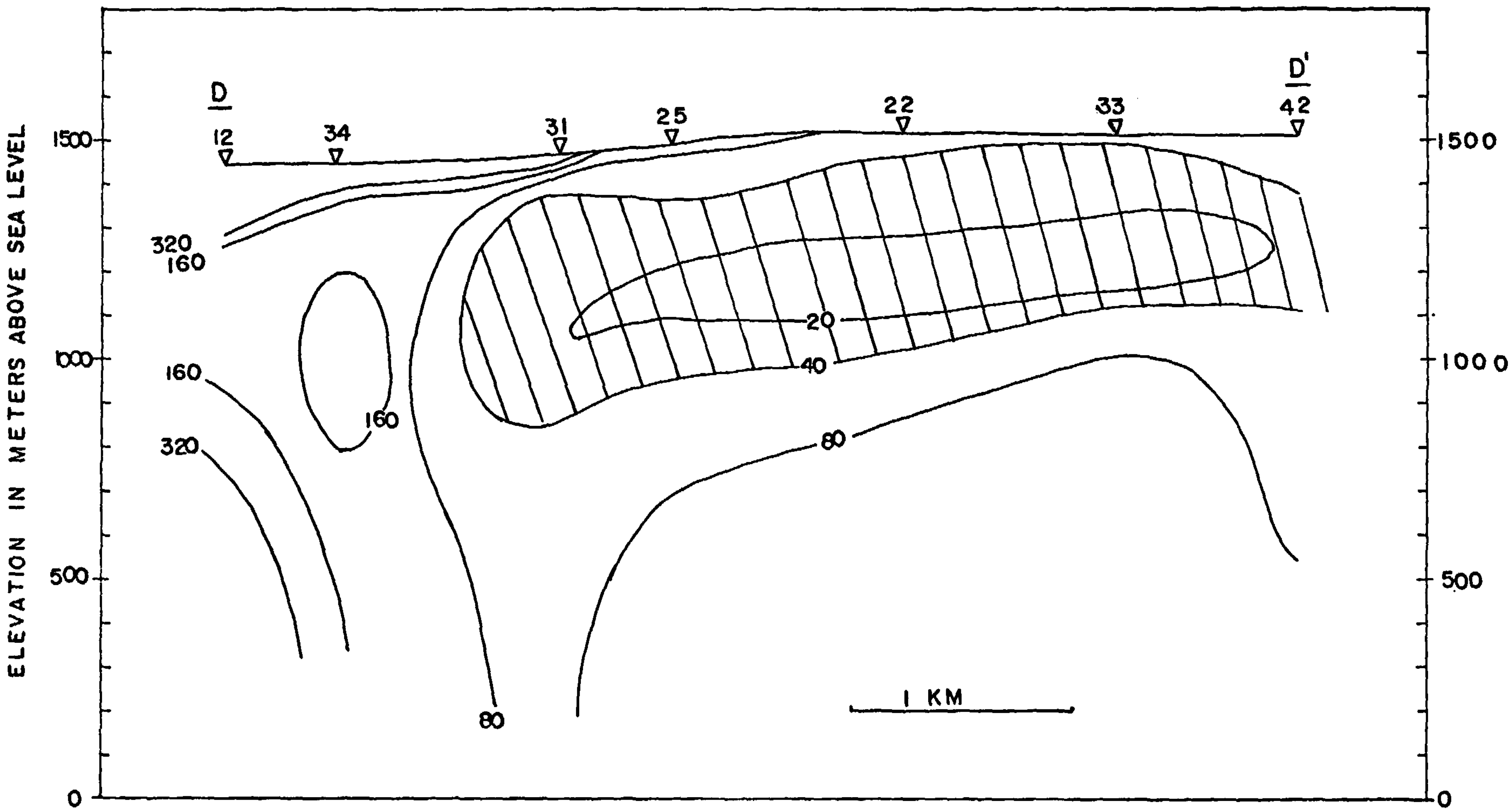

Figure 6.--Geoelectric cross-section D-D' (fig. 1) compiled from interpreted resistivity sounding data. Contours increase in geometric progession from a value of 20 ohm-meters. Patterned areas are those intervals considered to be composed primarily of argillaceous argillite of the Eleana Formation. Vertical exaggeration is 2X.

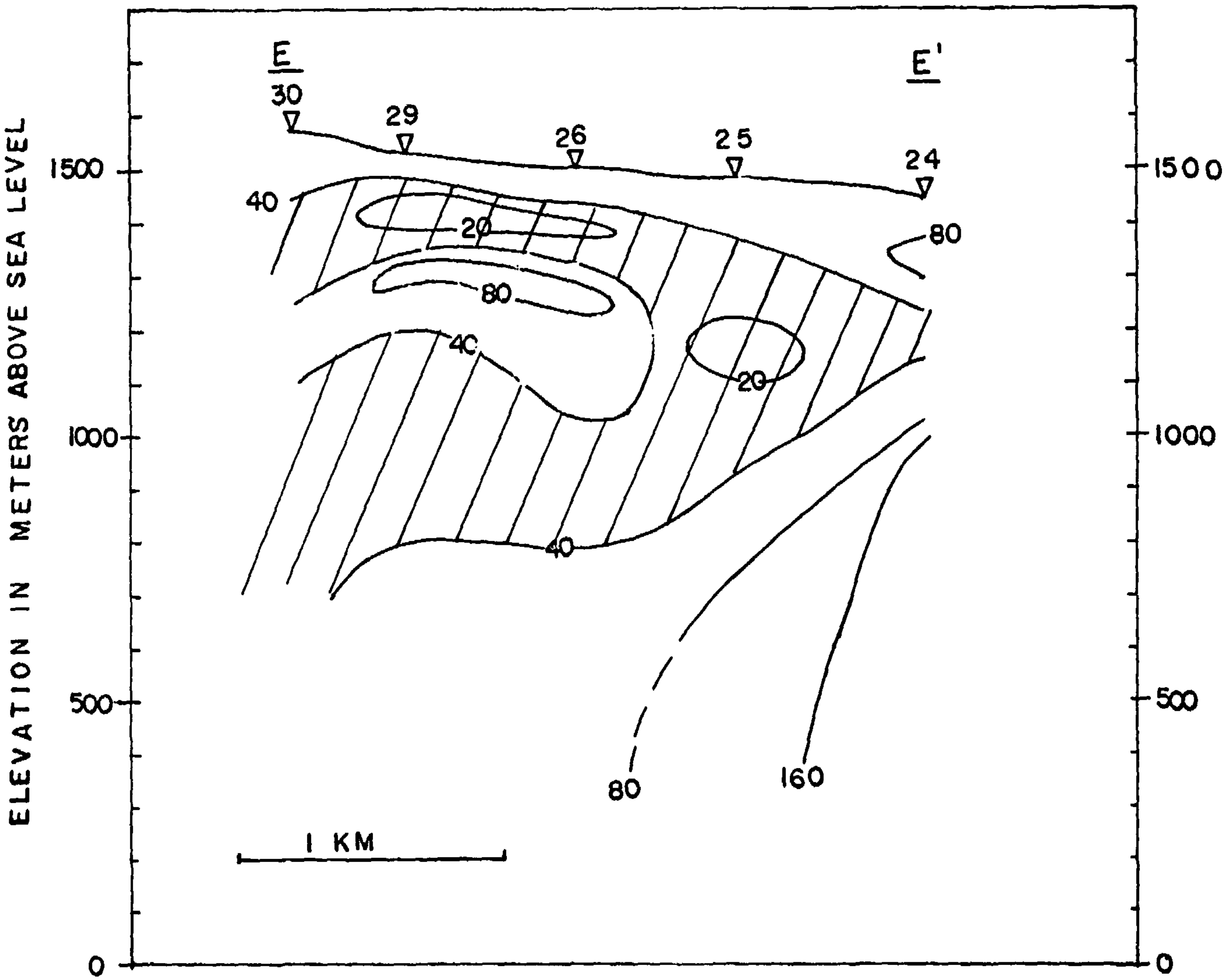

Figure 7.--Geoelectric cross-section E-E (fig. 1) compiled from interpreted resistivity sounding data. Contours increase in geometric progression from a value of 20 ohm-meters. Dashed contours indicate inferred values of resistivity. Patterned areas are those intervals considered to be composed primarily of argillaceous argillite of the Eleana Formation. Vertical exaggeration is 2X.

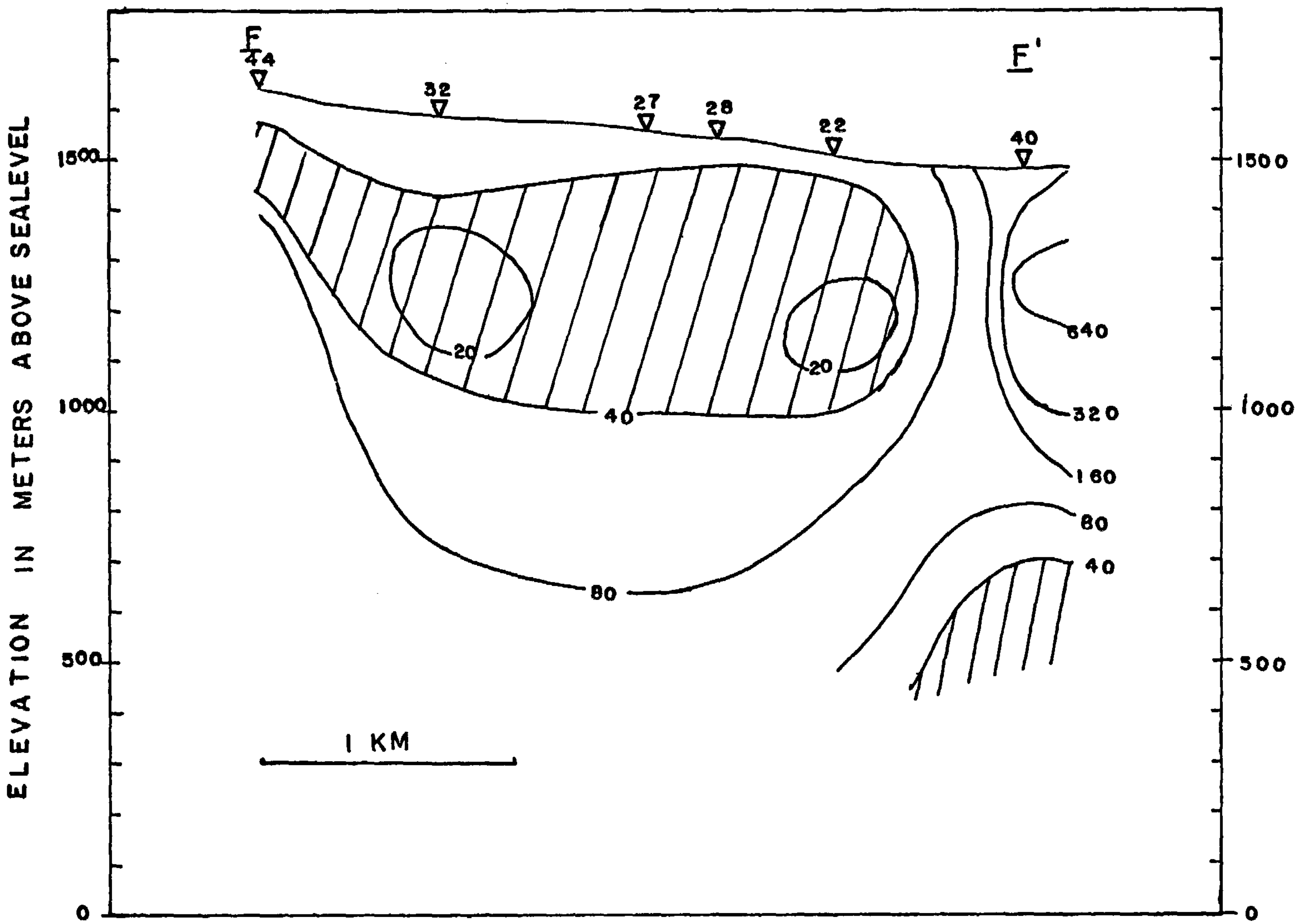

Figure 8.--Geoelectric cross-section F-F' (fig. 1) compiled from interpreted resistivity sounding data. Contours increase in geometric progrssion from a value of 20 ohm-meters. Patterned areas are those intervals considered to be composed primarily of argillaceous argillite of the Eleana Formation. Vertical exaggeration is 2X.

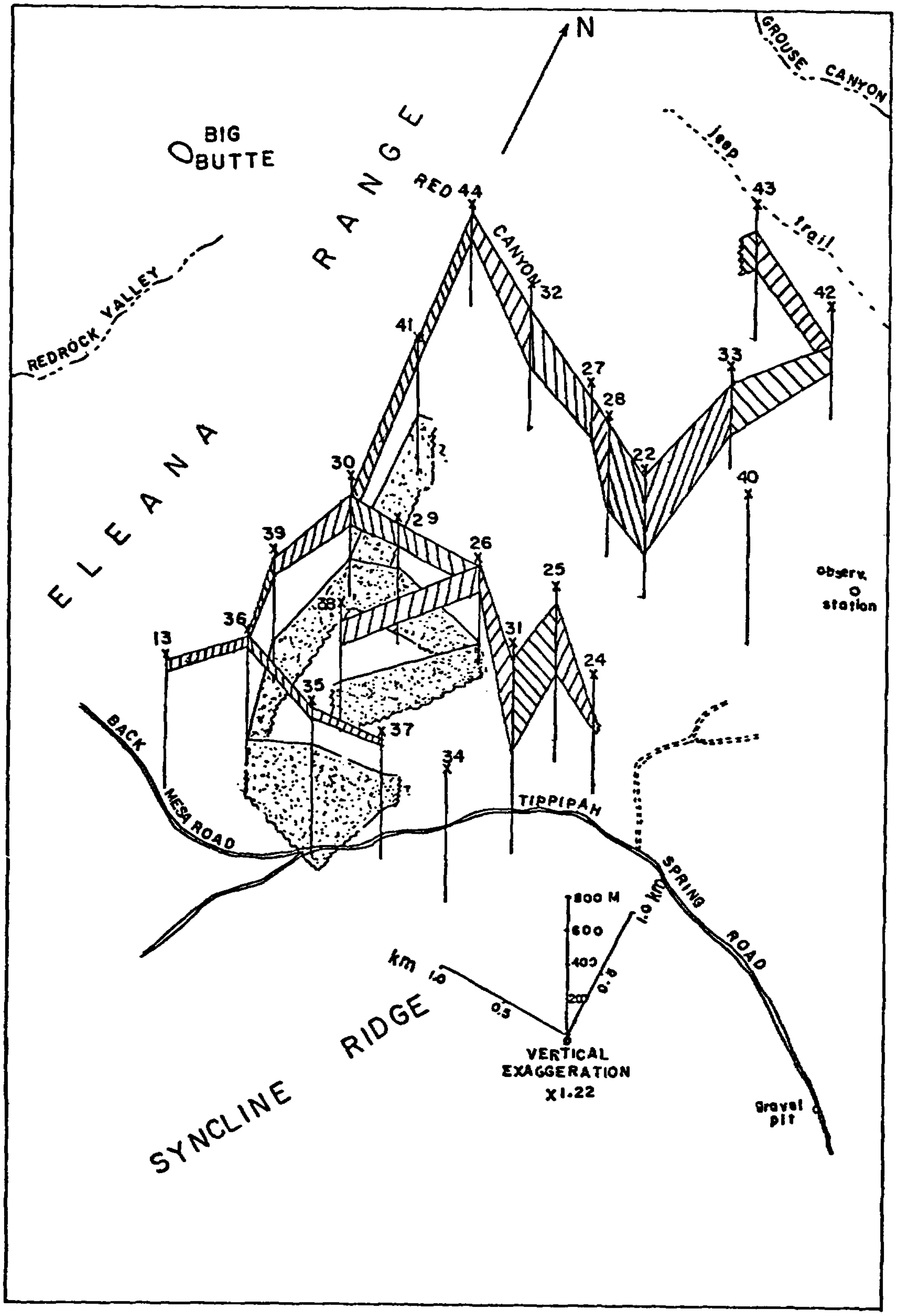

Figure 9.--Fense diagram constructed to show the distribution of rock interpreted to be primarily argillaceous argillite of the Eleana Formation (<40 ohm-meters, shown in both hachured and stippled patterns) within the area lying between the Eleana Range and the northern extension of Syncline Ridge. The X's mark the geographic location of the respective Schlumberger soundings and the lines extending below the X's indicate the depth to which the resistivity data could be interpreted.

Appendix

Vertical electrical soundings Eleana 1 through 44. On each curve the measured field data are represented by diamonds connected by straight line segments; the squares denote a shifted field curve obtained by vertical adjustment of individual segments relative to the right-hand segment of the sounding curves; and the plus symbols are theoretical data points obtained for the interpreted geoelectric section. The geoelectric section is represented by the columnar graph which indicates the resistivity and thickness of individual layers with increasing depth. The dotted profile is the corresponding Dar Zarrouk curve for the interpreted geoelectric section.

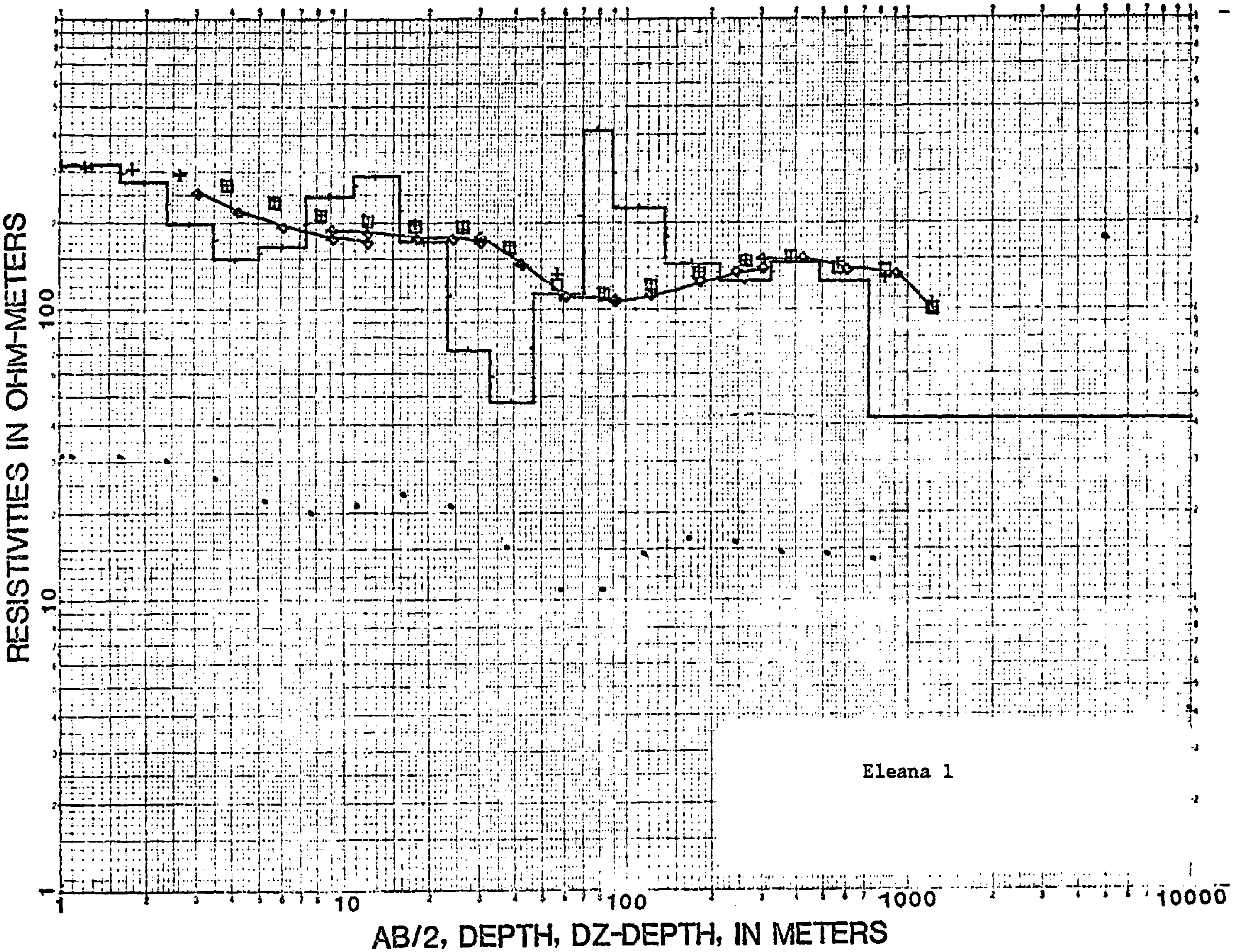

RESISTIVITIES IN OHM-METERS
100
10
1
10
100
1000
10000
AB/2, DEPTH, DZ-DEPTH, IN METERS
Eleana 1

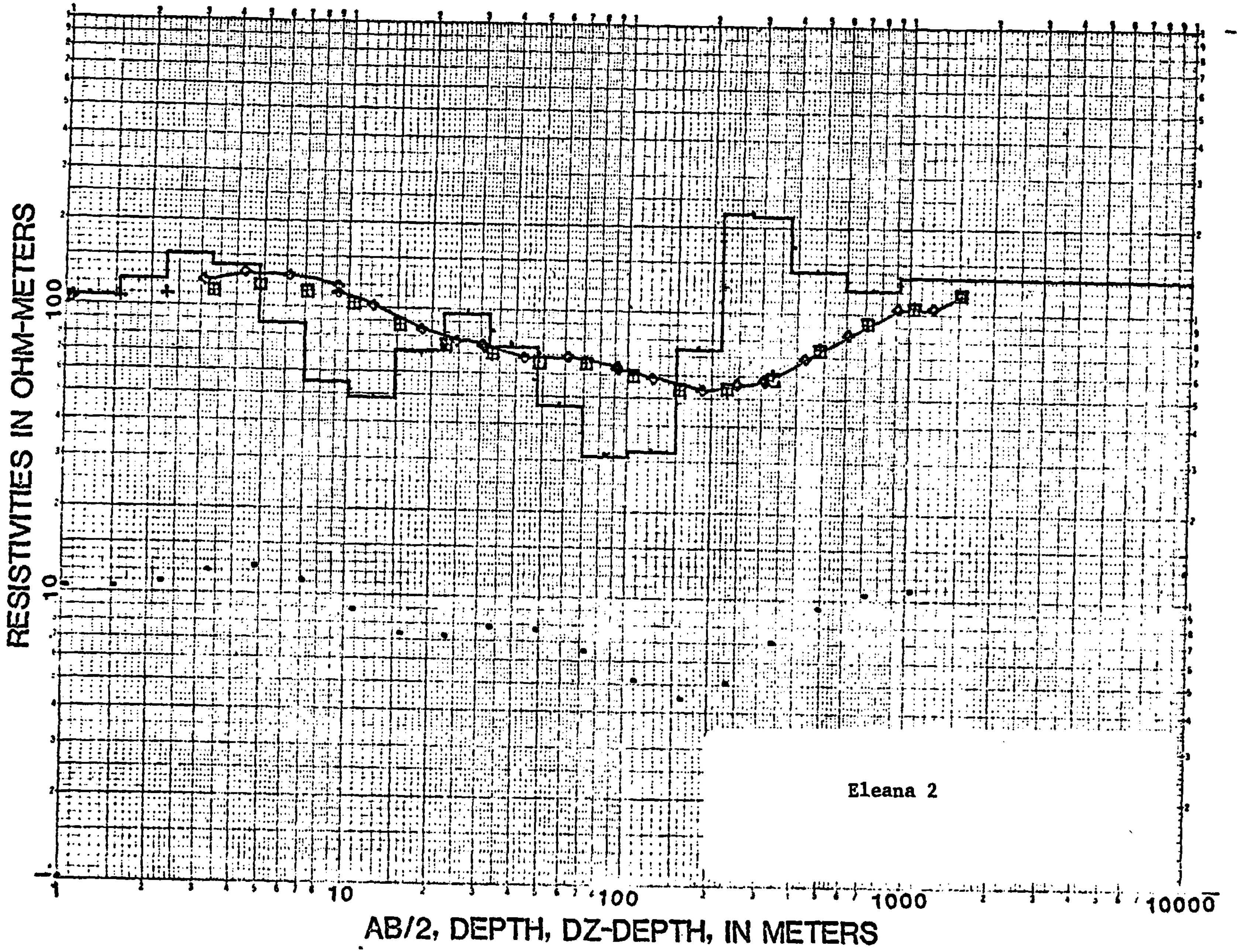

RESISTIVITIES IN OHM-METERS
100
10
1
10
100
1000
10000
AB/2, DEPTH, DZ-DEPTH, IN METERS
Eleana 2

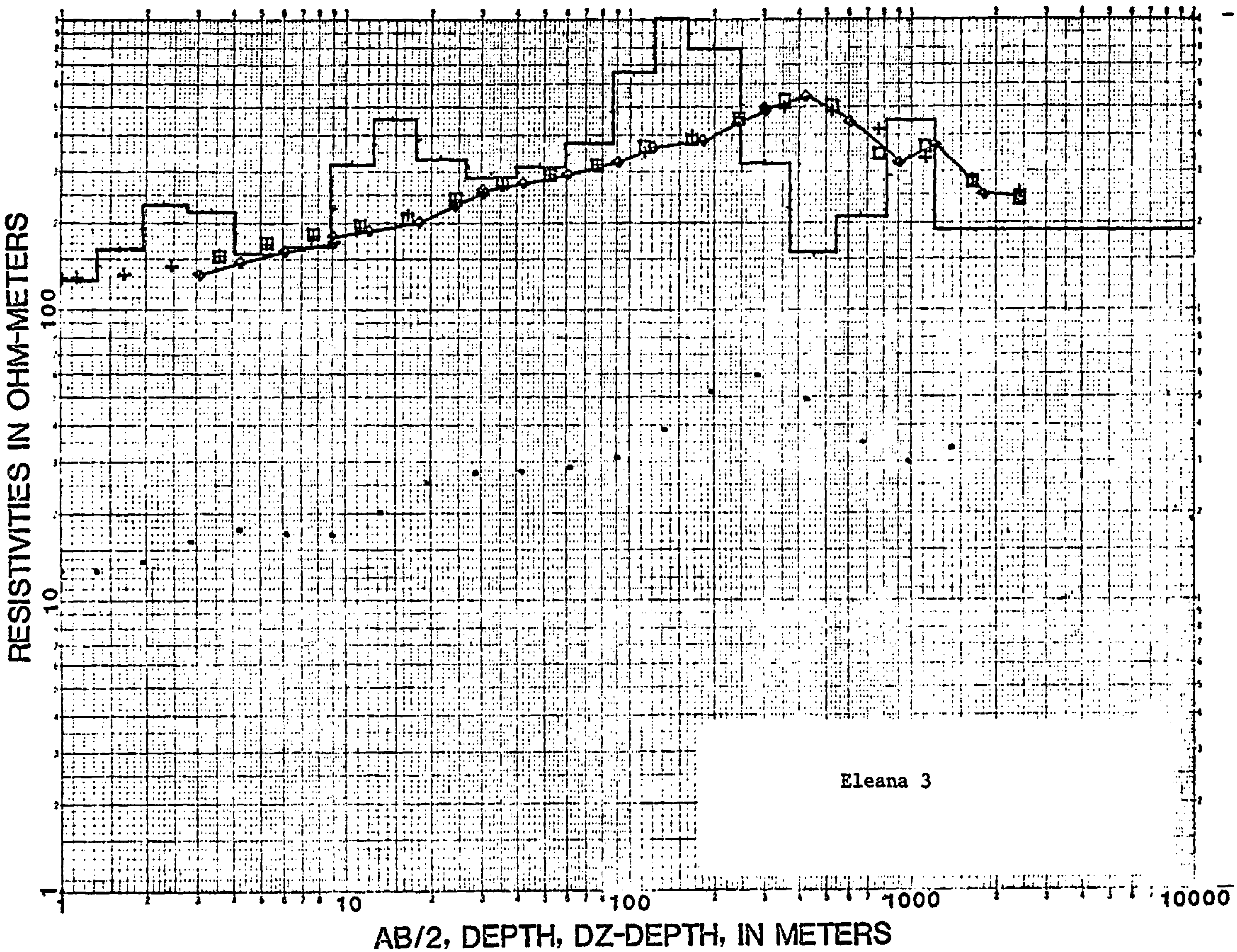
RESISTIVITIES IN OHM-METERS
100
10
1
10
100
1000
10000
AB/2, DEPTH, DZ-DEPTH, IN METERS
Eleana 3

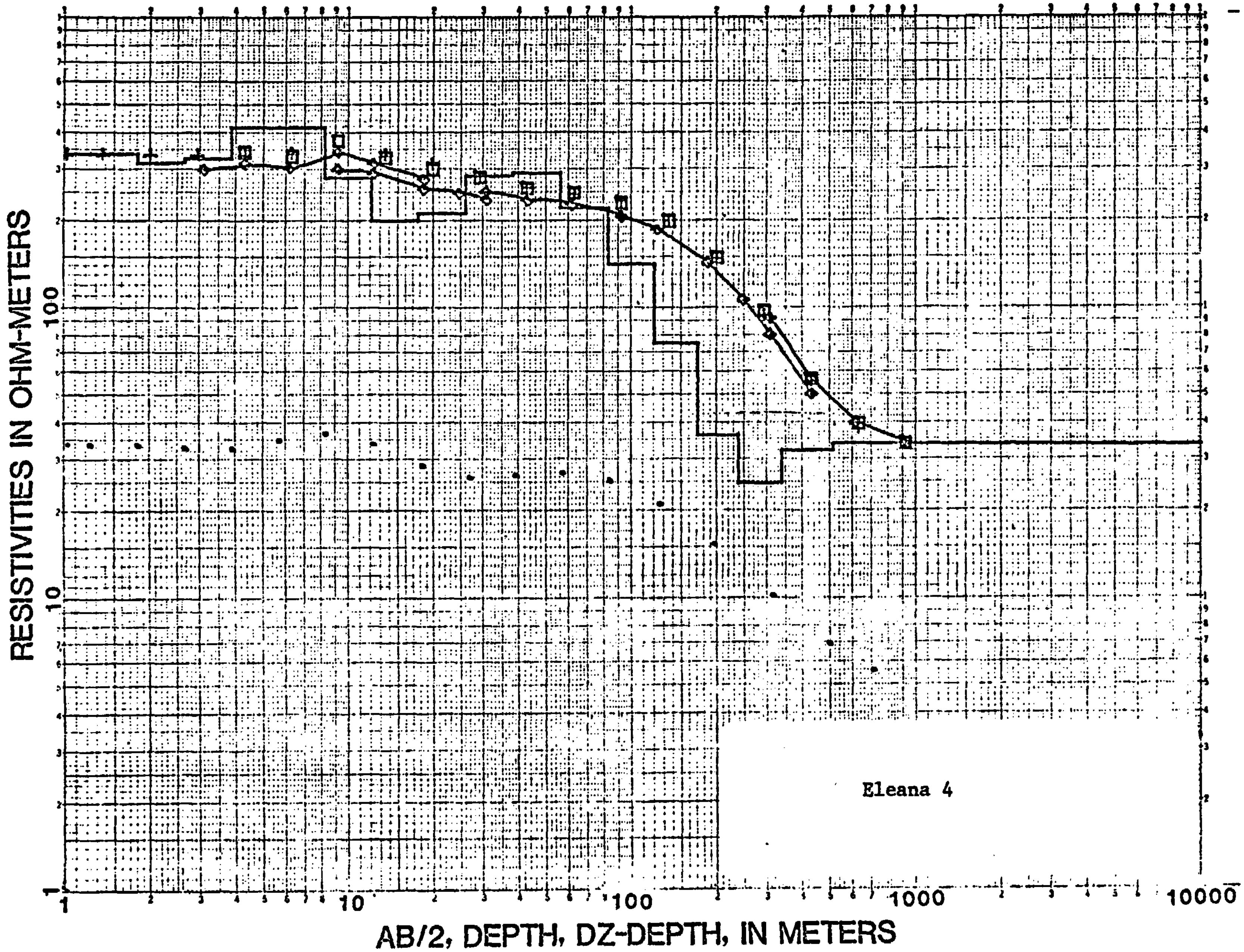

RESISTIVITIES IN OHM-METERS
100
10
1
10
100
1000
10000
AB/2, DEPTH, DZ-DEPTH, IN METERS
Eleana 4

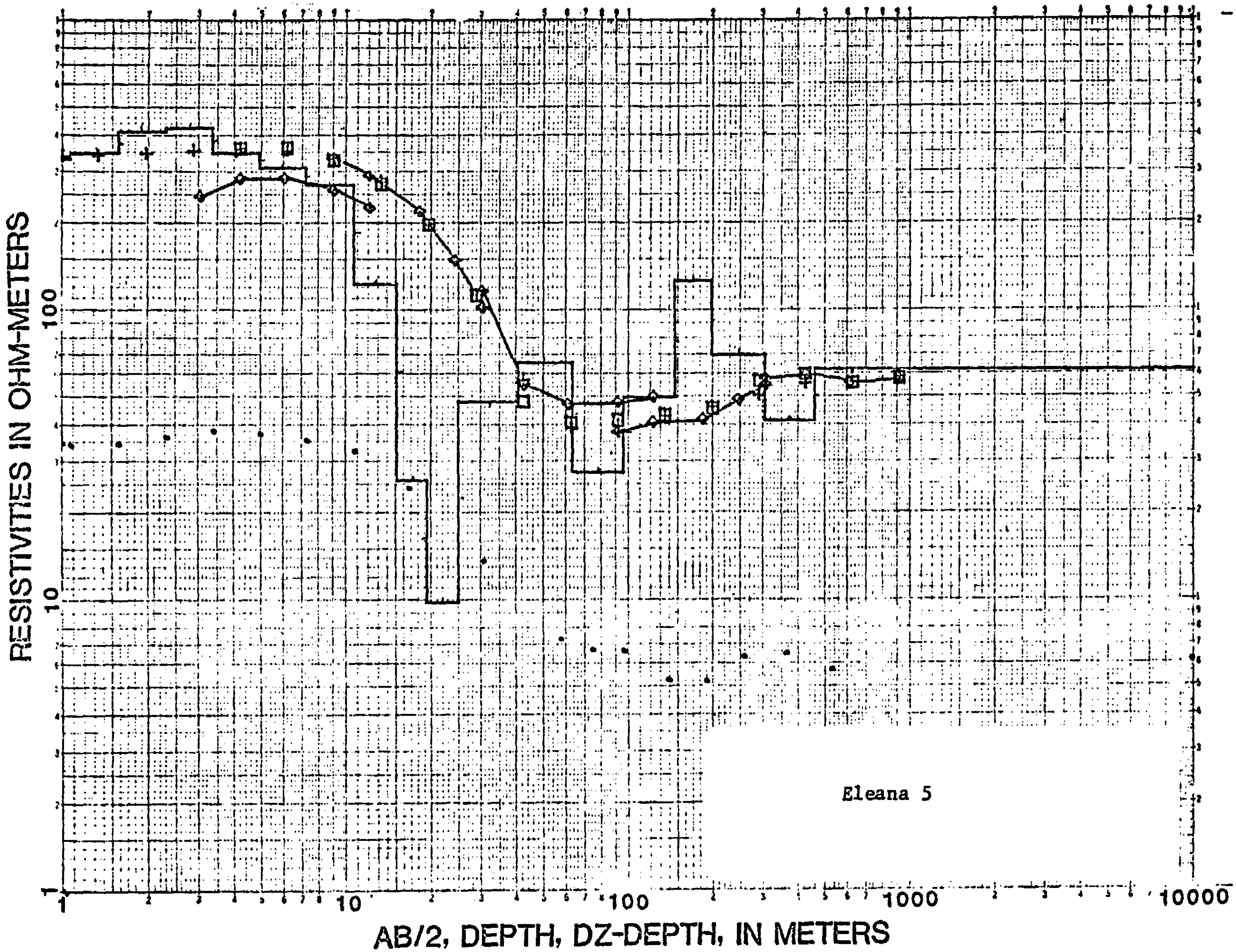

RESISTIVITIES IN OHM-METERS
100
10
1
10
100
1000
10000
AB/2, DEPTH, DZ-DEPTH, IN METERS
Eleana 5

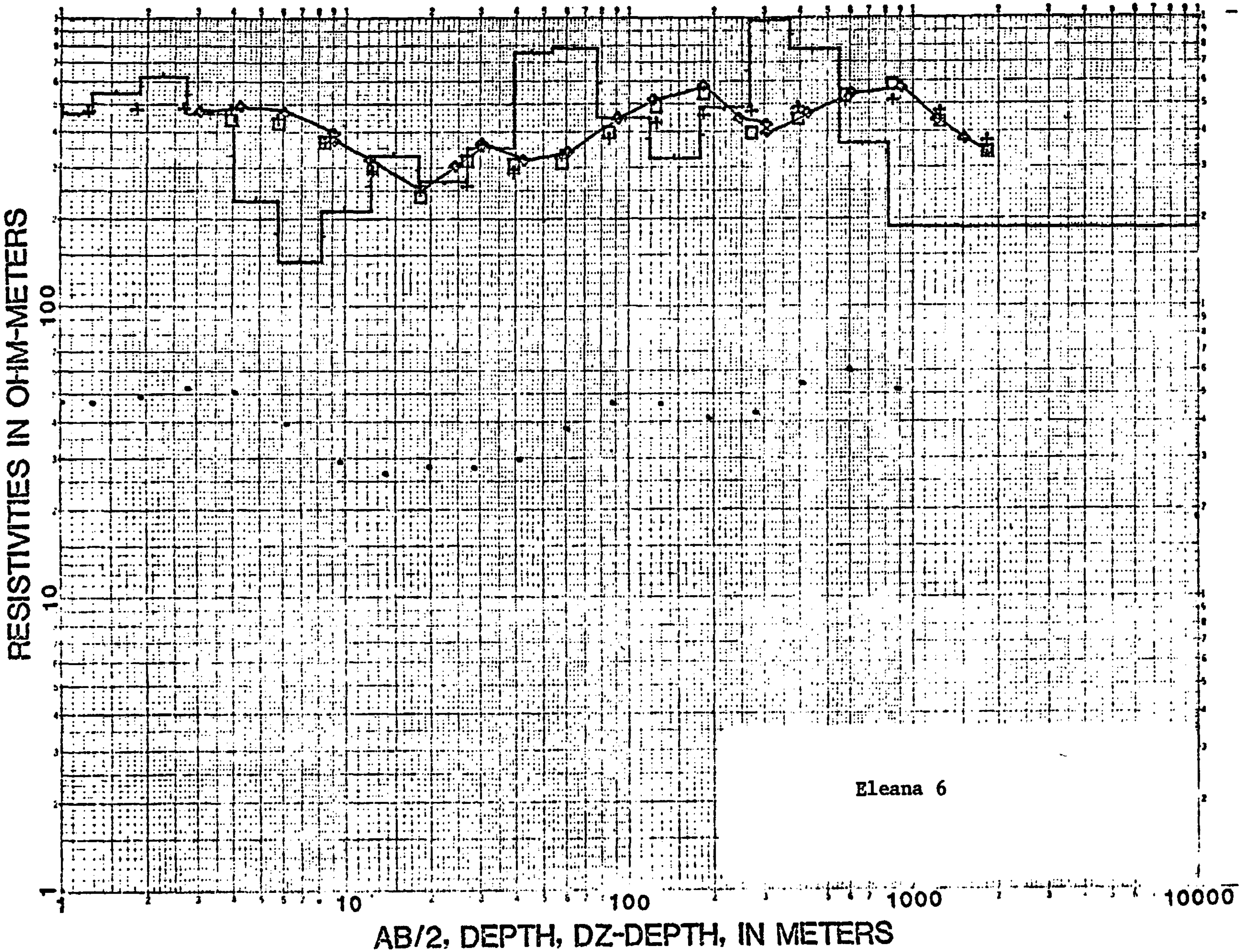

RESISTIVITIES IN OHM-METERS
100
10
1
10
100
1000
10000
AB/2, DEPTH, DZ-DEPTH, IN METERS
Eleana 6

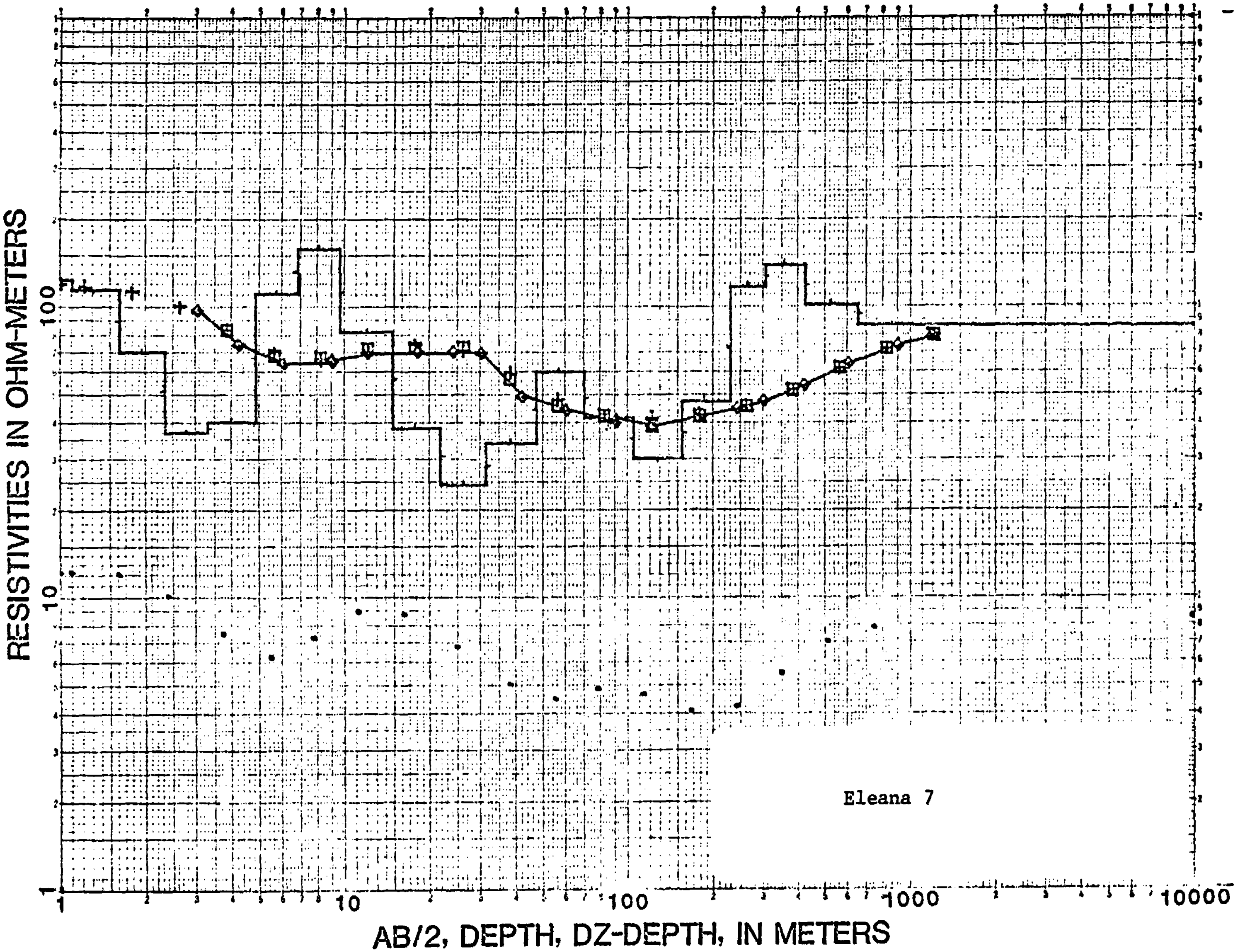
RESISTIVITIES IN OHM-METERS
AB/2, DEPTH, DZ-DEPTH, IN METERS
1
10
100
1000
10000
Eleana 7

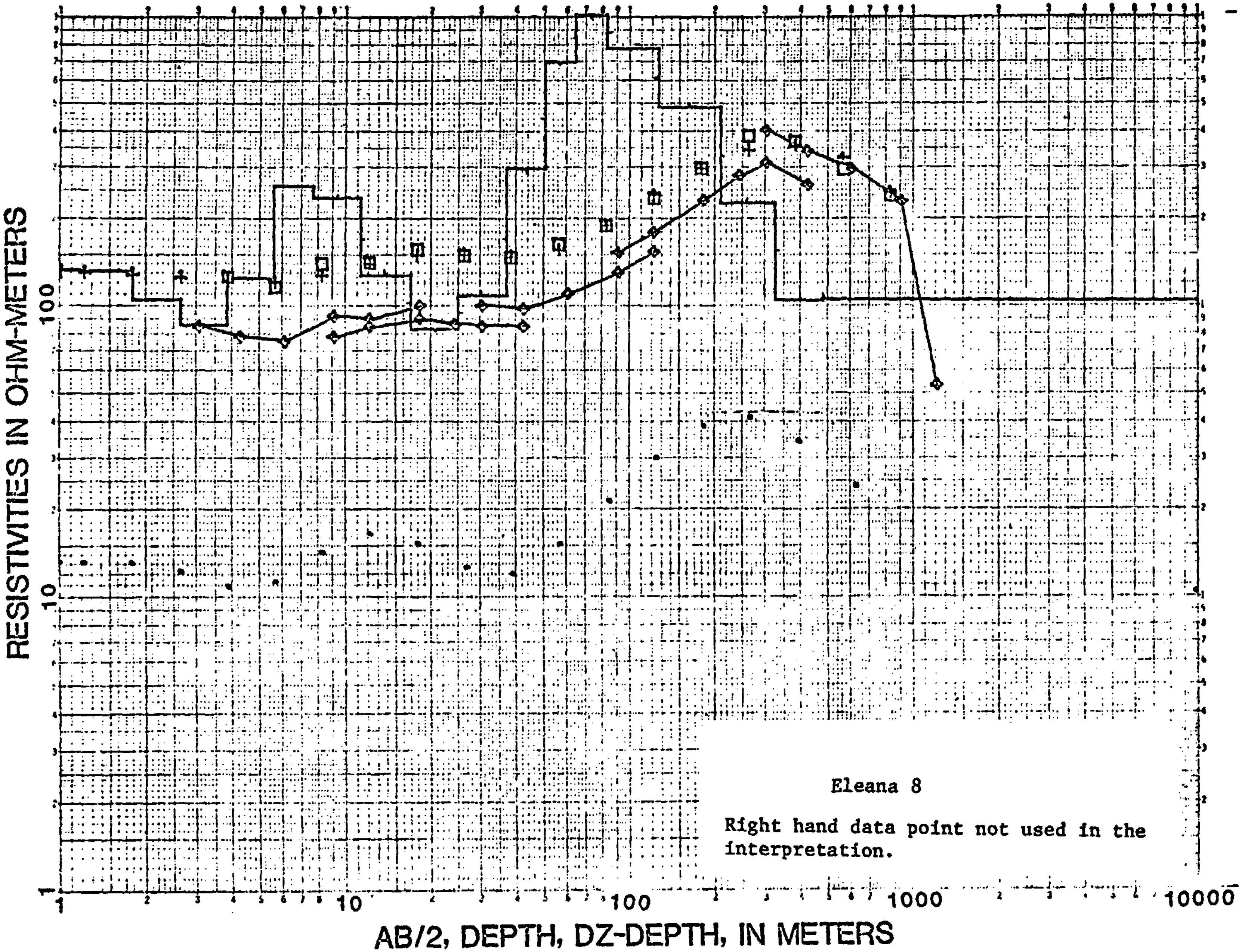
RESISTIVITIES IN OHM-METERS
100
10
1
10
100
1000
10000
AB/2, DEPTH, DZ-DEPTH, IN METERS
Eleana 8
Right hand data point not used in the interpretation.

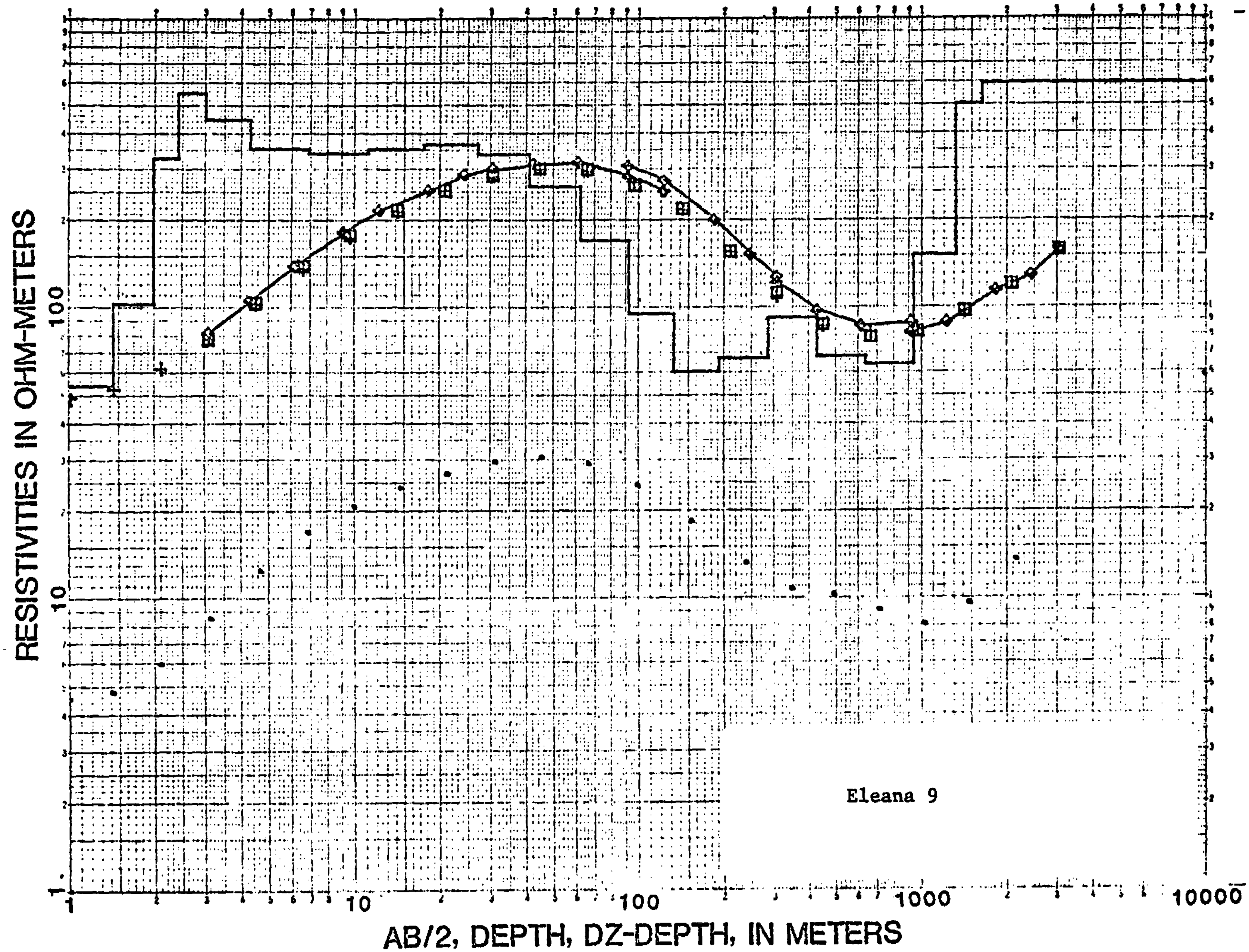
RESISTIVITIES IN OHM-METERS
100
10
1
10
100
1000
10000
AB/2, DEPTH, DZ-DEPTH, IN METERS
Eleana 9

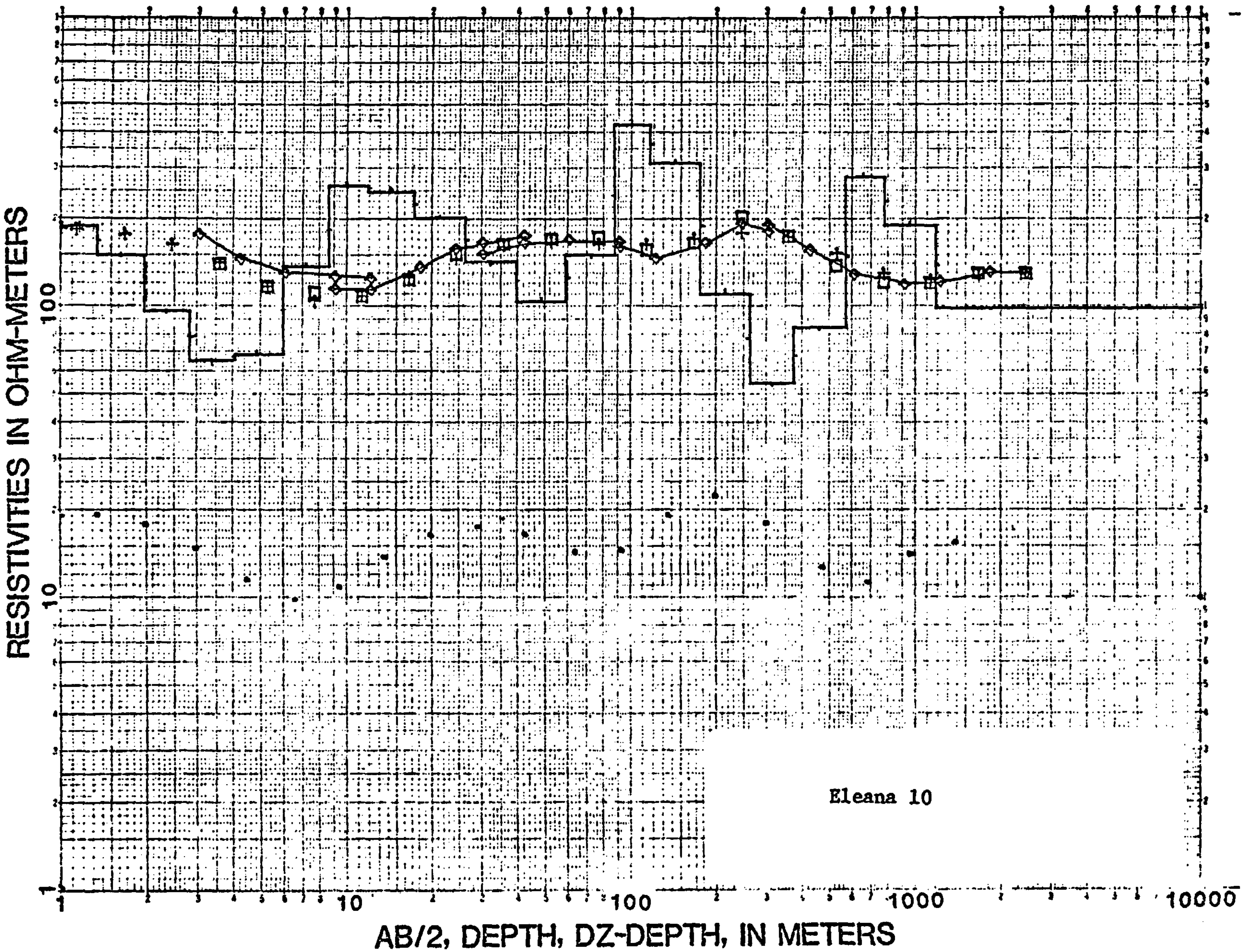
RESISTIVITIES IN OHM-METERS
100
10
AB/2, DEPTH, DZ-DEPTH, IN METERS
1
10
100
1000
10000
Eleana 10

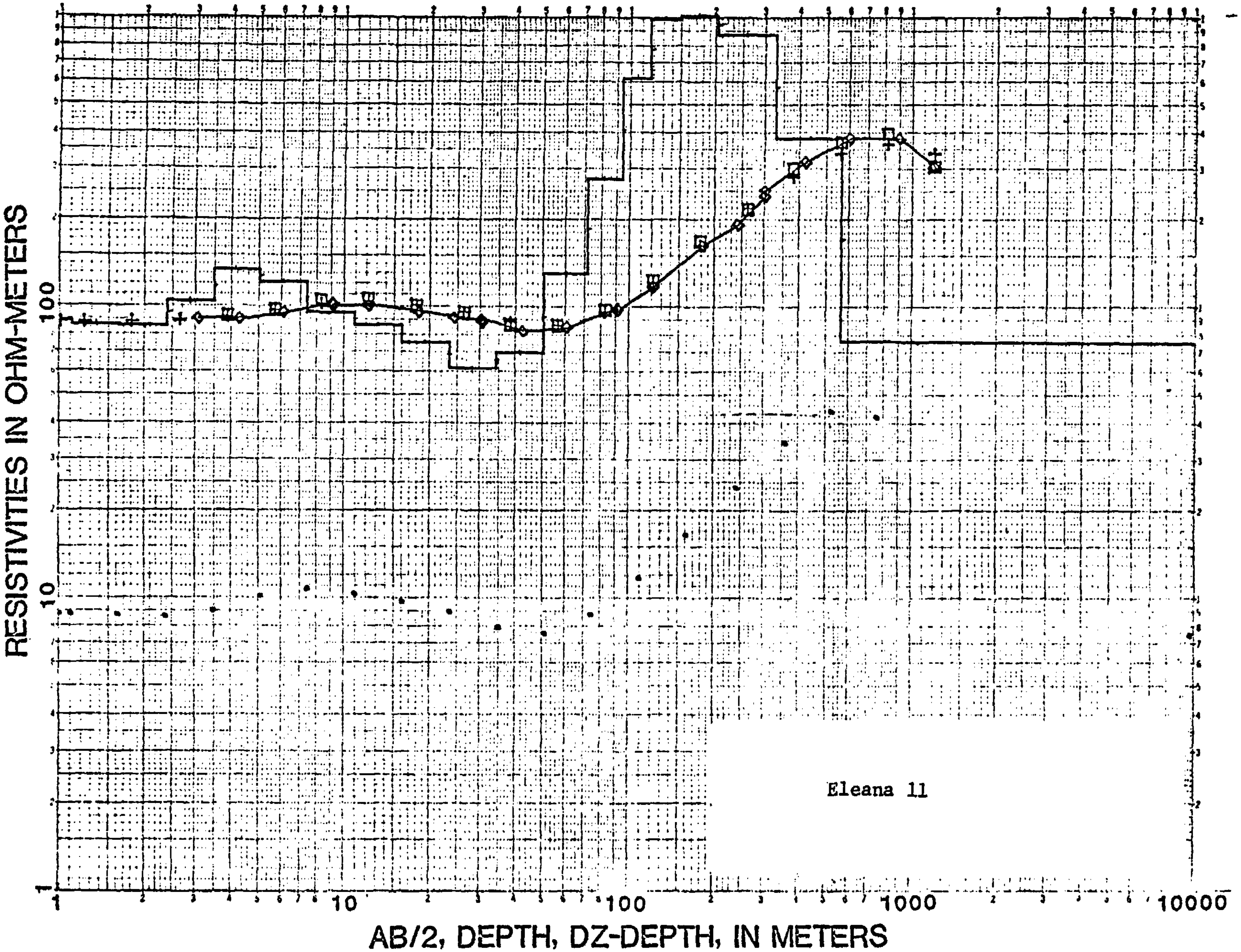

RESISTIVITIES IN OHM-METERS
100
10
1
10
100
1000
10000
AB/2, DEPTH, DZ-DEPTH, IN METERS
Eleana 11

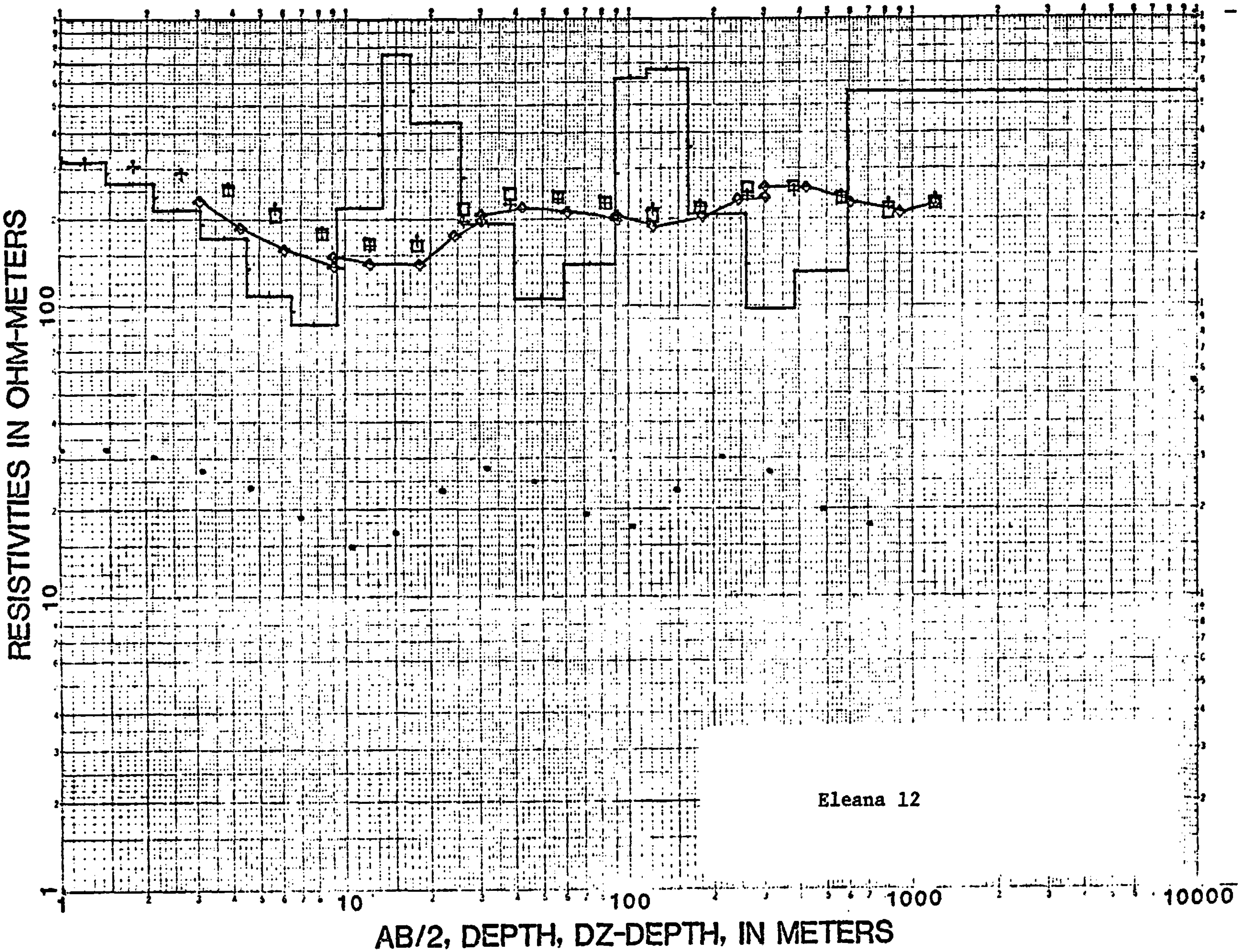
RESISTIVITIES IN OHM-METERS
100
10
1
10
100
1000
10000
AB/2, DEPTH, DZ-DEPTH, IN METERS
Eleana 12

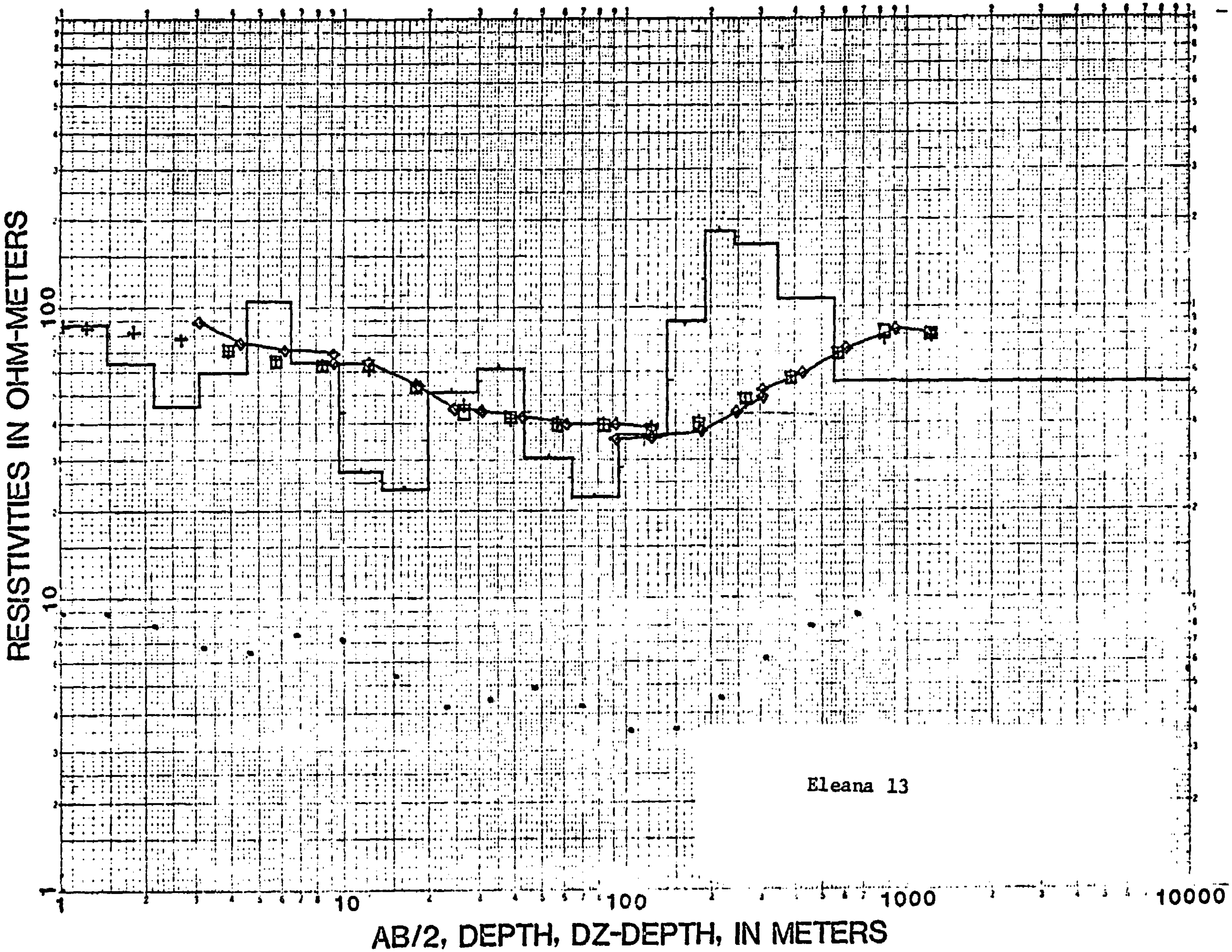
RESISTIVITIES IN OHM-METERS
100
10
1
10
100
1000
10000
AB/2, DEPTH, DZ-DEPTH, IN METERS
Eleana 13

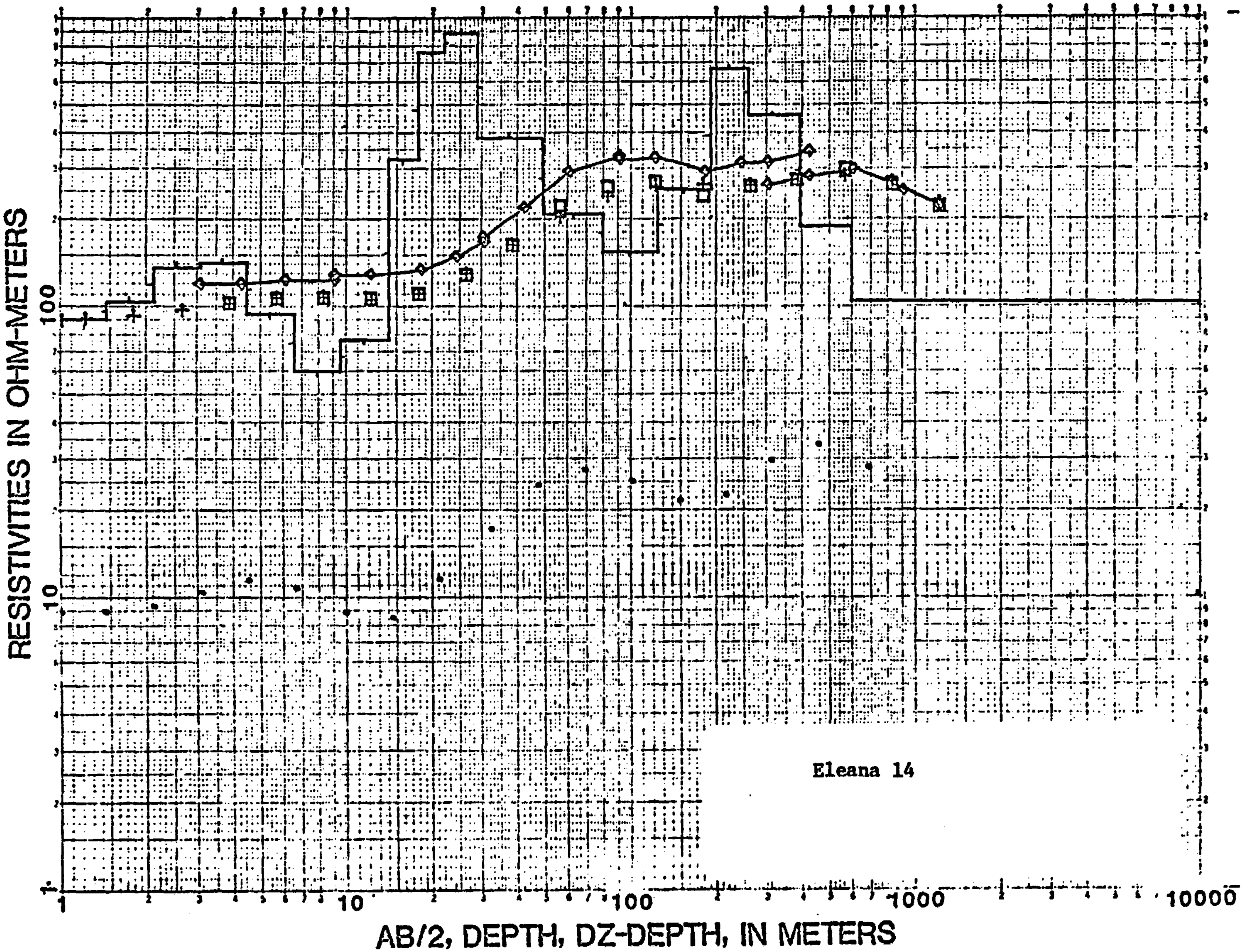
RESISTIVITIES IN OHM-METERS
100
10
1
10
100
1000
10000
AB/2, DEPTH, DZ-DEPTH, IN METERS
Eleana 14

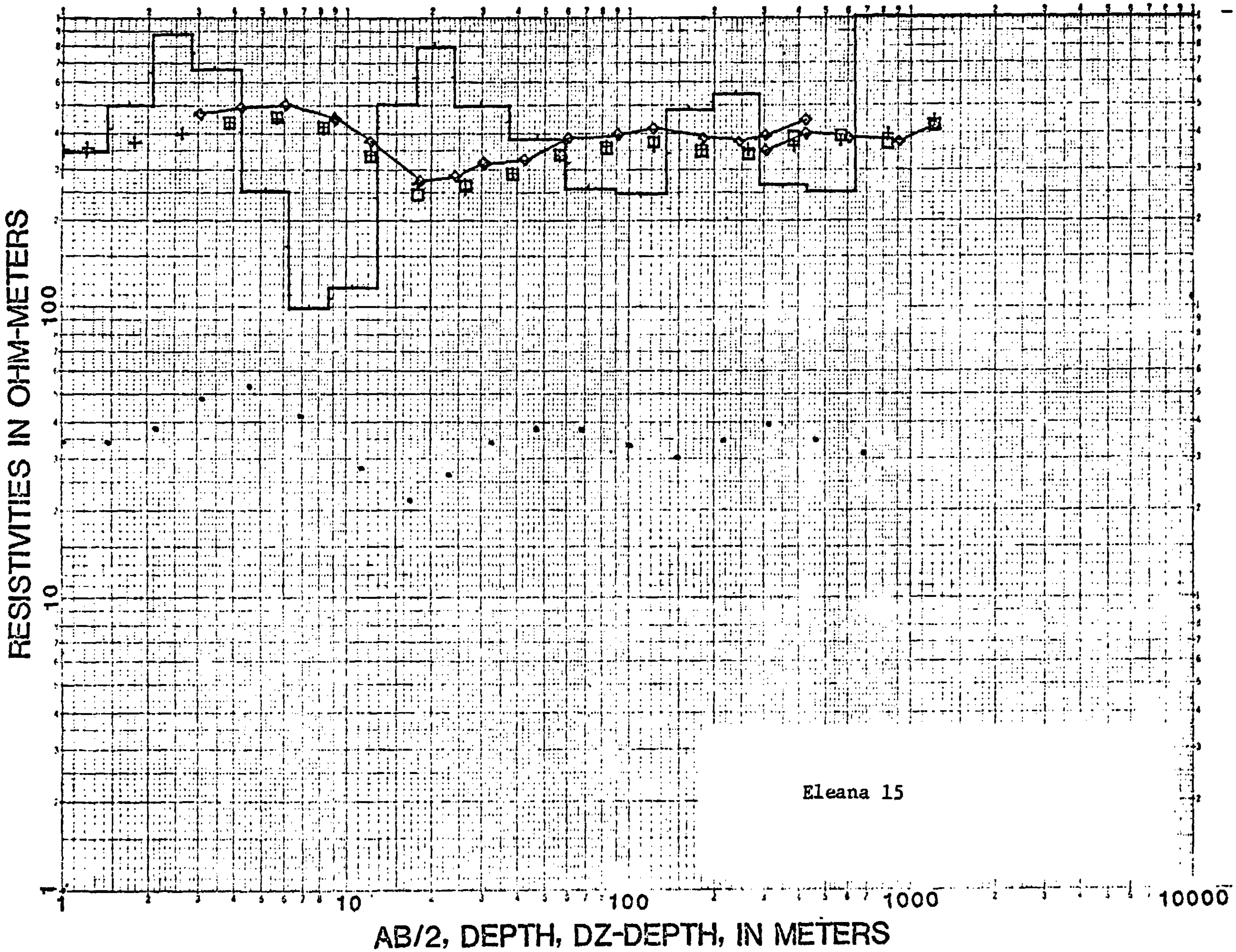
RESISTIVITIES IN OHM-METERS
100
10
1
1
10
100
1000
10000
AB/2, DEPTH, DZ-DEPTH, IN METERS
Eleana 15

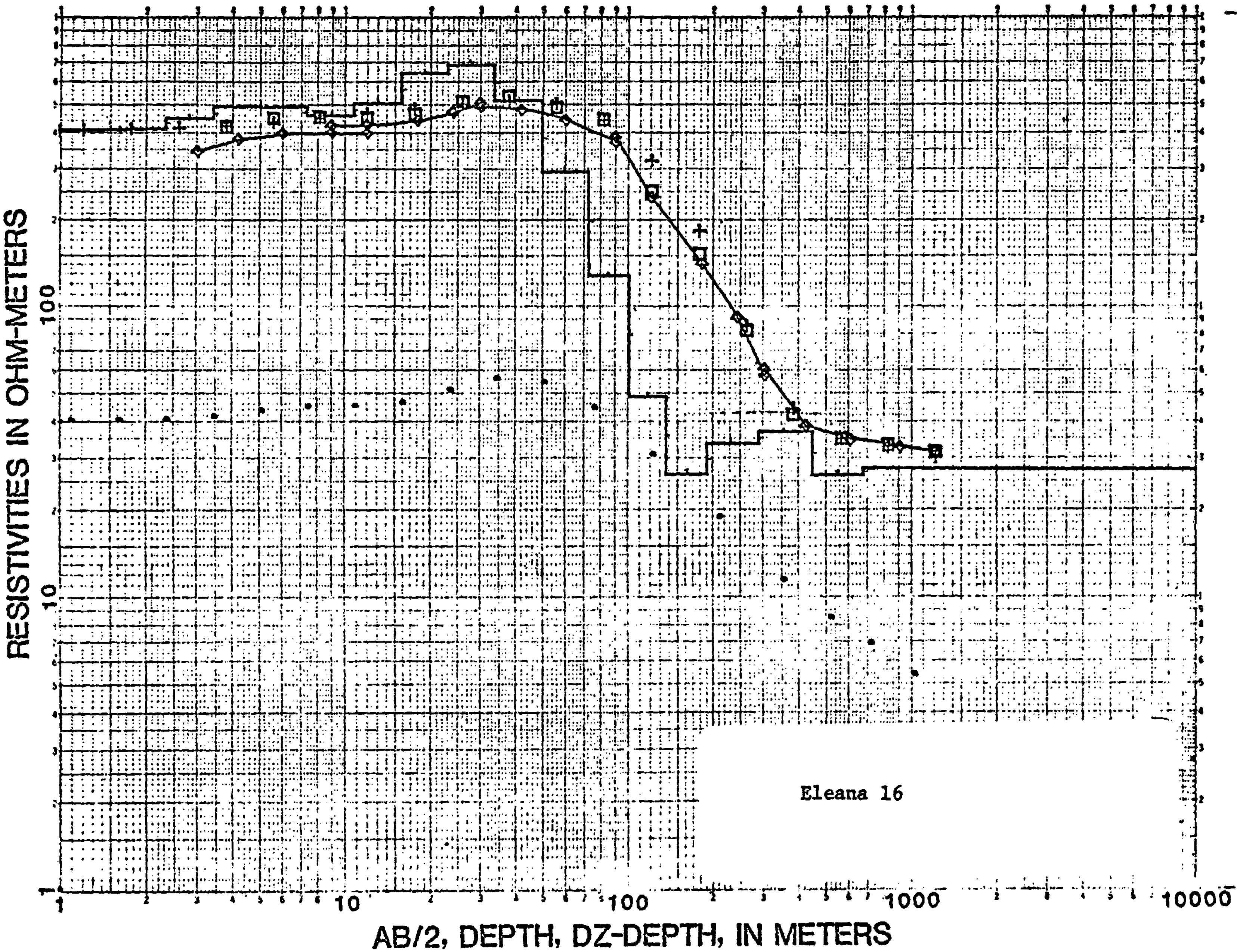
RESISTIVITIES IN OHM-METERS
100
10
1
10
100
1000
10000
AB/2, DEPTH, DZ-DEPTH, IN METERS
Eleana 16

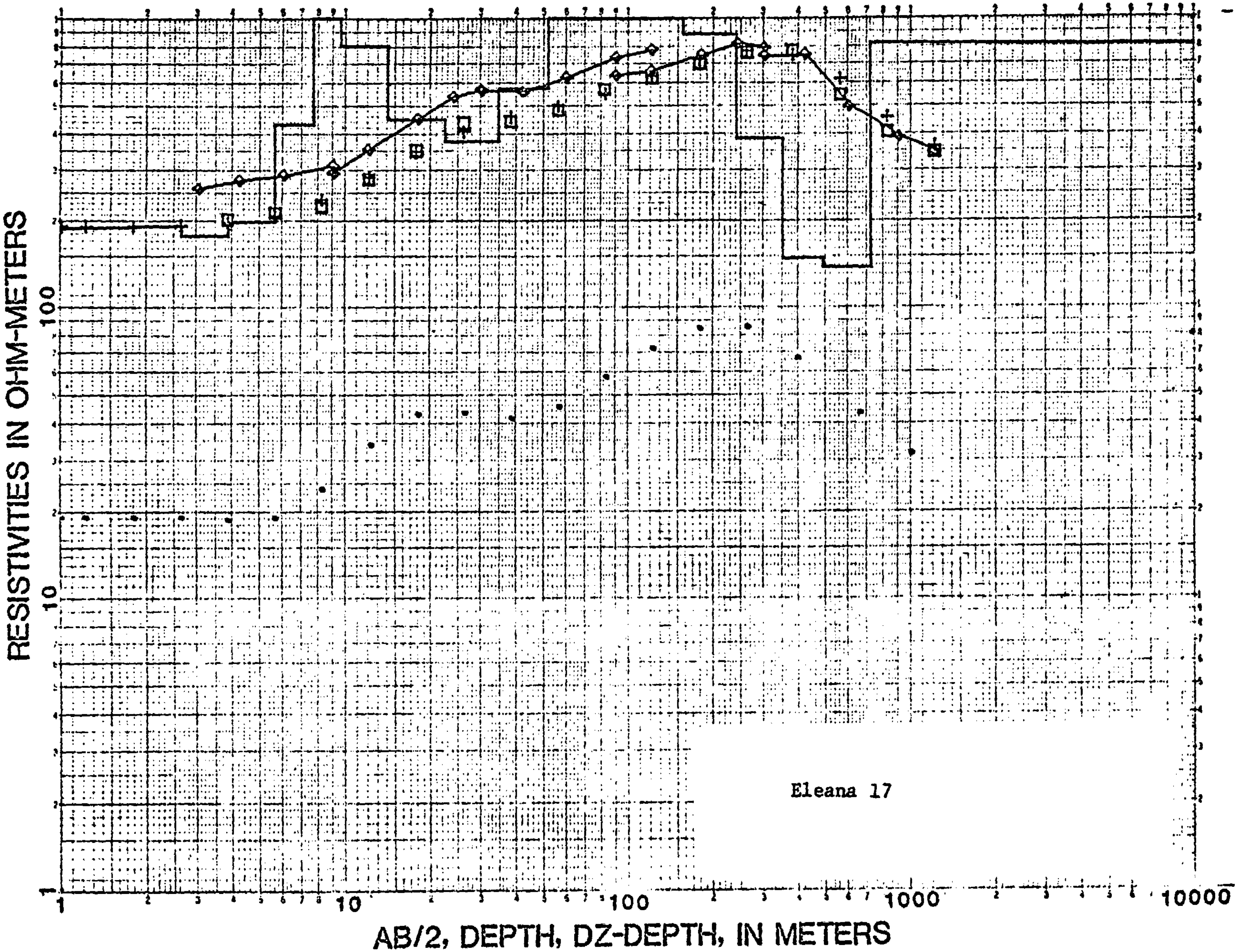

RESISTIVITIES IN OHM-METERS
100
10
1
1
10
100
1000
10000
AB/2, DEPTH, DZ-DEPTH, IN METERS
Eleana 17

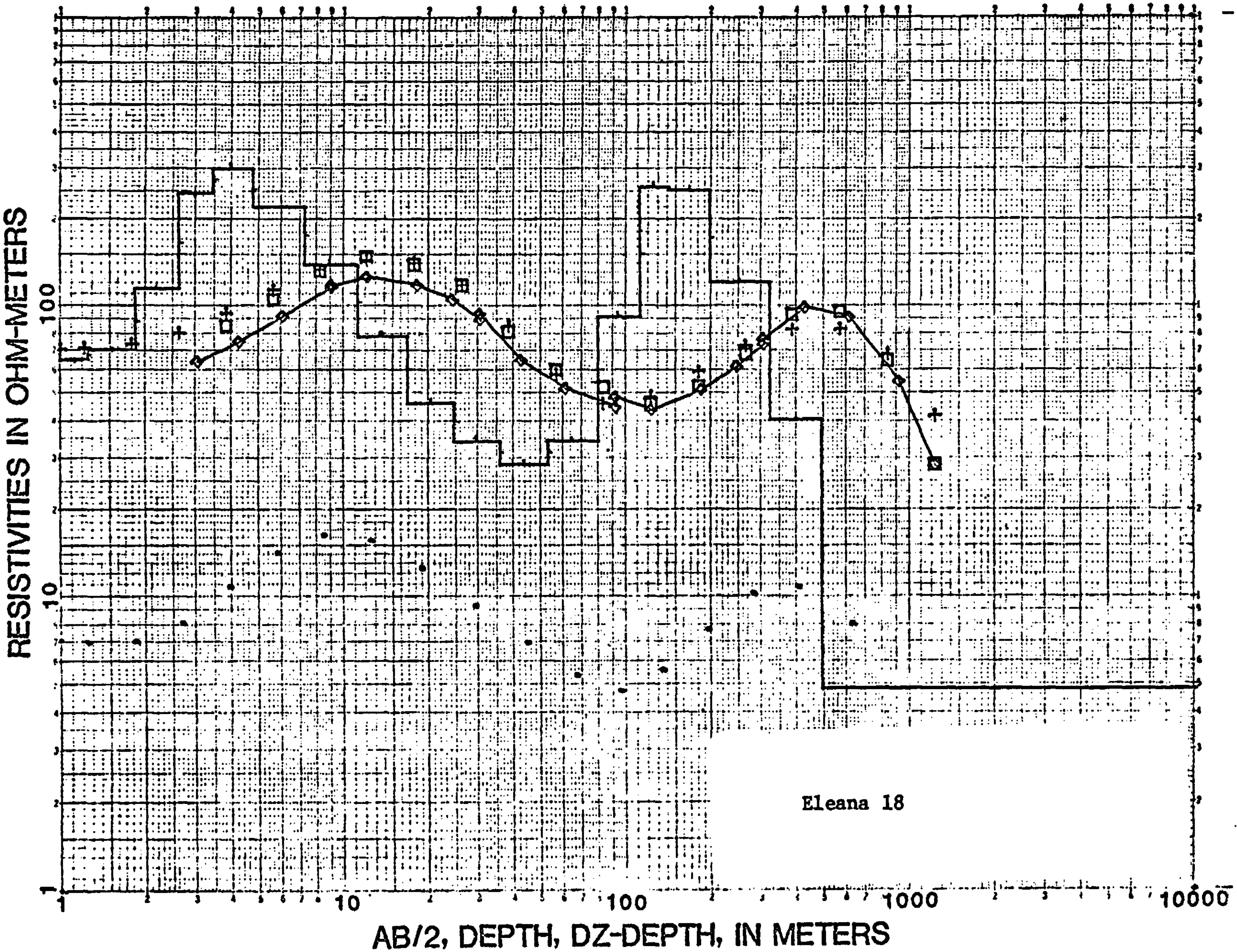
RESISTIVITIES IN OHM-METERS
100
10
1
10
100
1000
10000
AB/2, DEPTH, DZ-DEPTH, IN METERS
Eleana 18

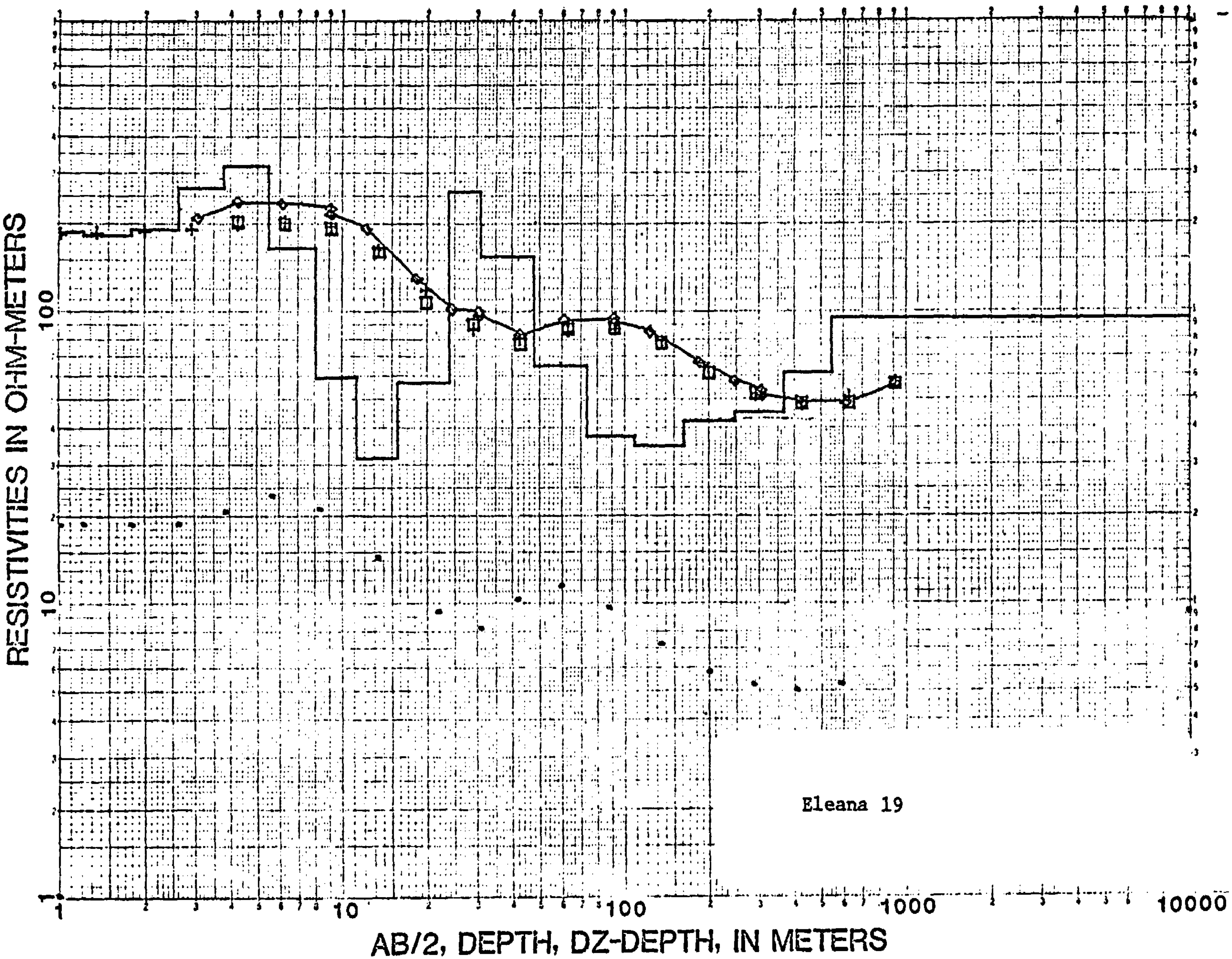

RESISTIVITIES IN OHM-METERS
100
10
1
10
100
1000
10000
AB/2, DEPTH, DZ-DEPTH, IN METERS
Eleana 19

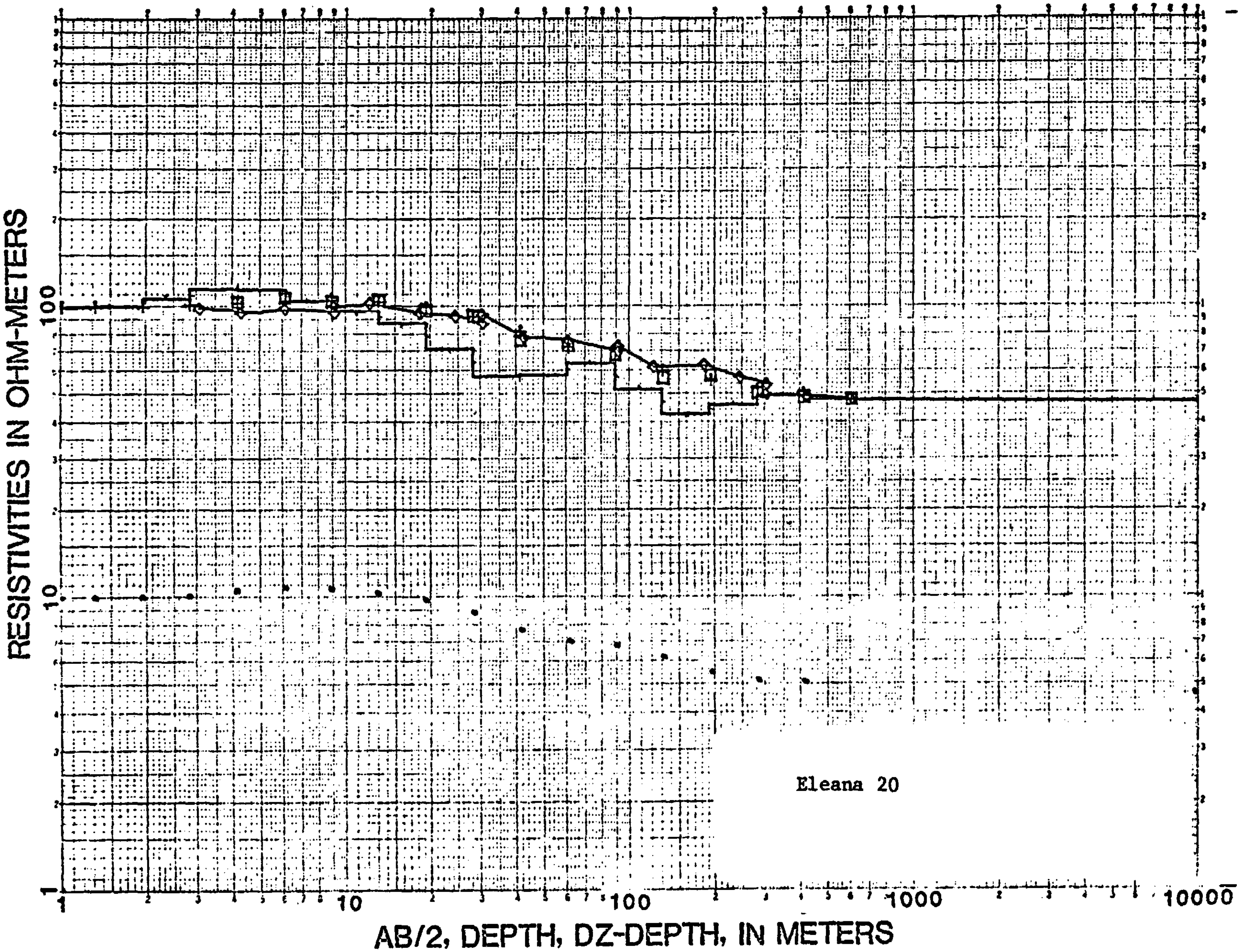

RESISTIVITIES IN OHM-METERS
100
10
1
10
100
1000
10000
AB/2, DEPTH, DZ-DEPTH, IN METERS
Eleana 20

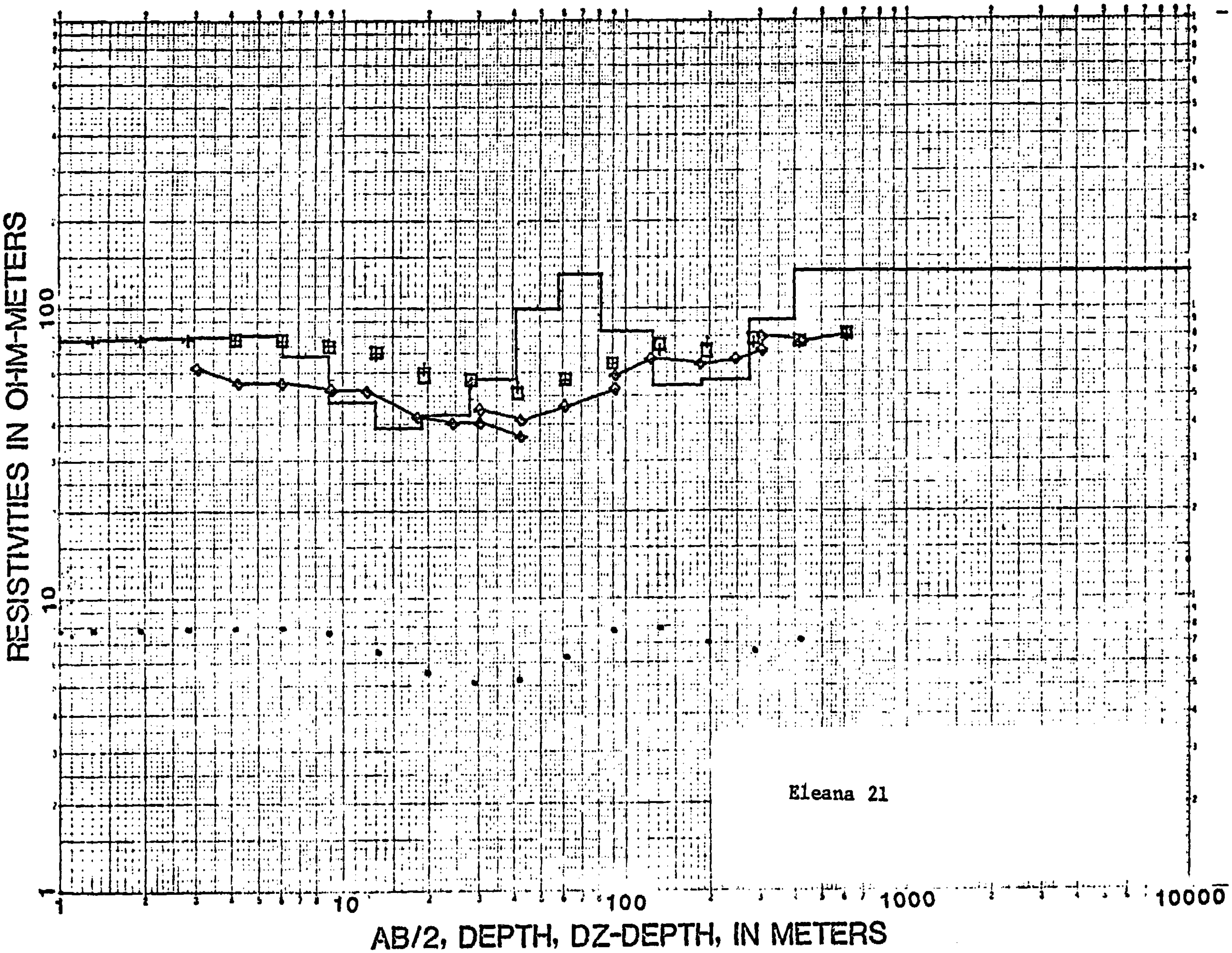

RESISTIVITIES IN OHM-METERS
100
10
1
10
100
1000
10000
AB/2, DEPTH, DZ-DEPTH, IN METERS
Eleana 21

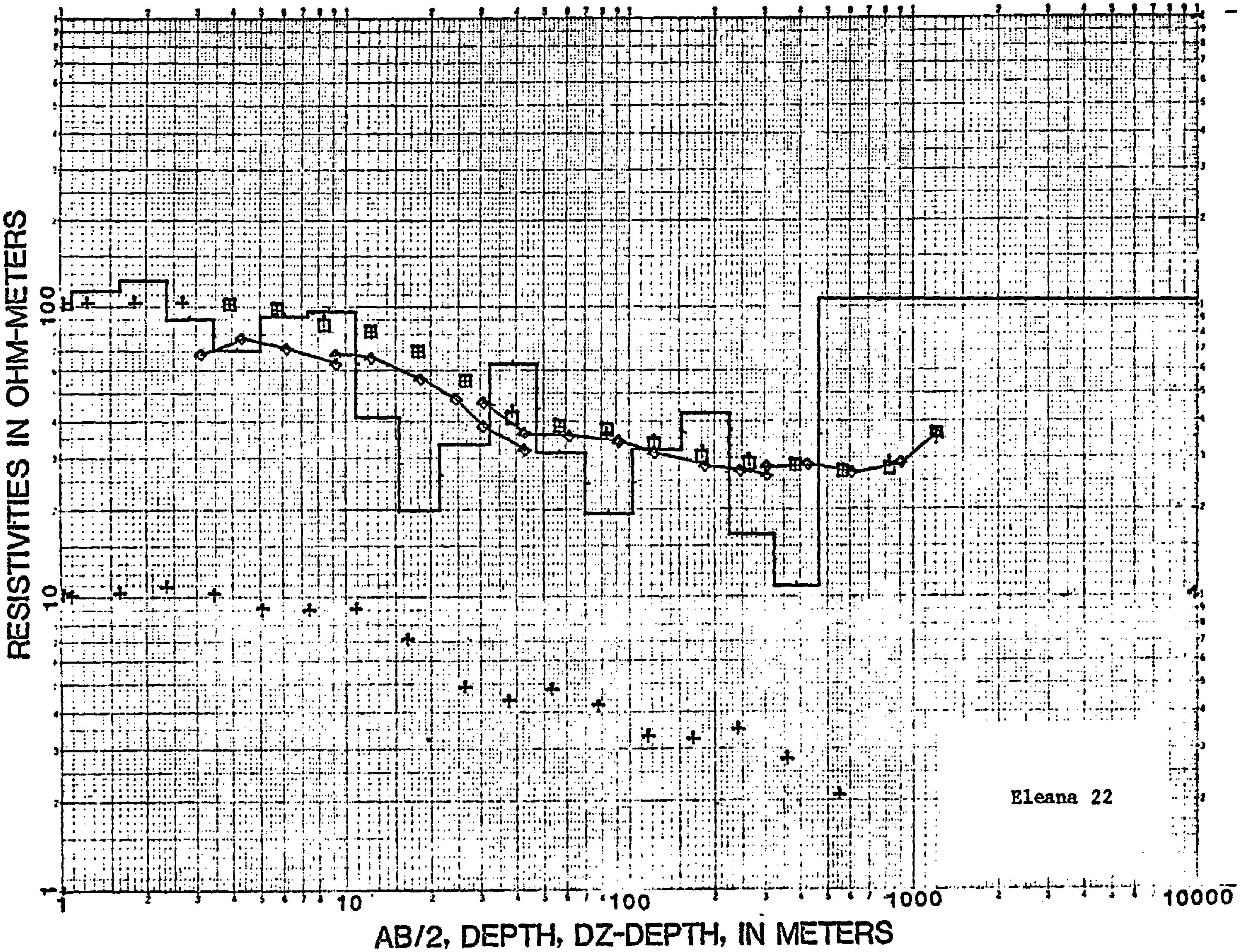

RESISTIVITIES IN OHM-METERS
100
10
1
10
100
1000
10000
AB/2, DEPTH, DZ-DEPTH, IN METERS
Eleana 22

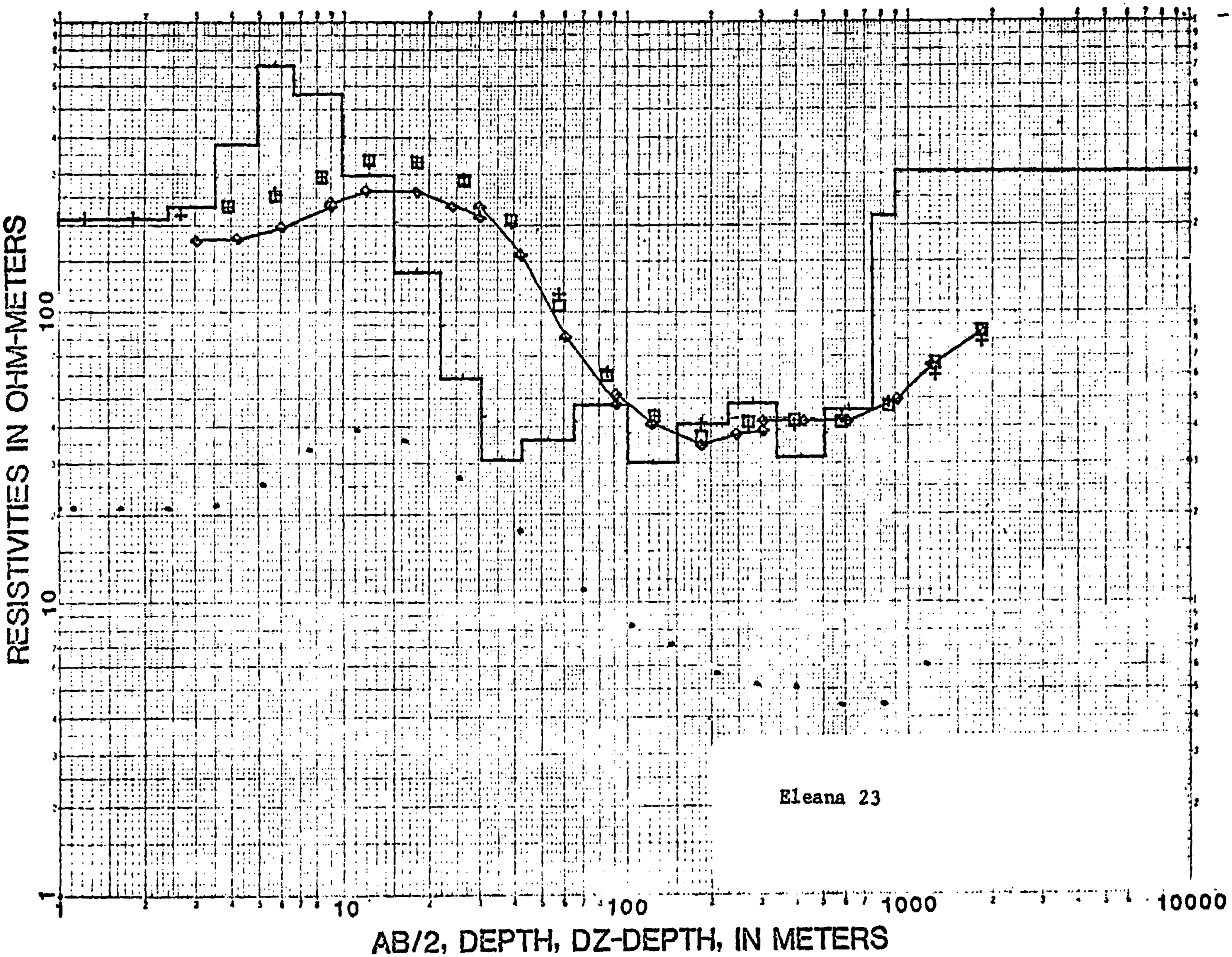

RESISTIVITIES IN OHM-METERS
1
10
100
1000
10000
AB/2, DEPTH, DZ-DEPTH, IN METERS
Eleana 23

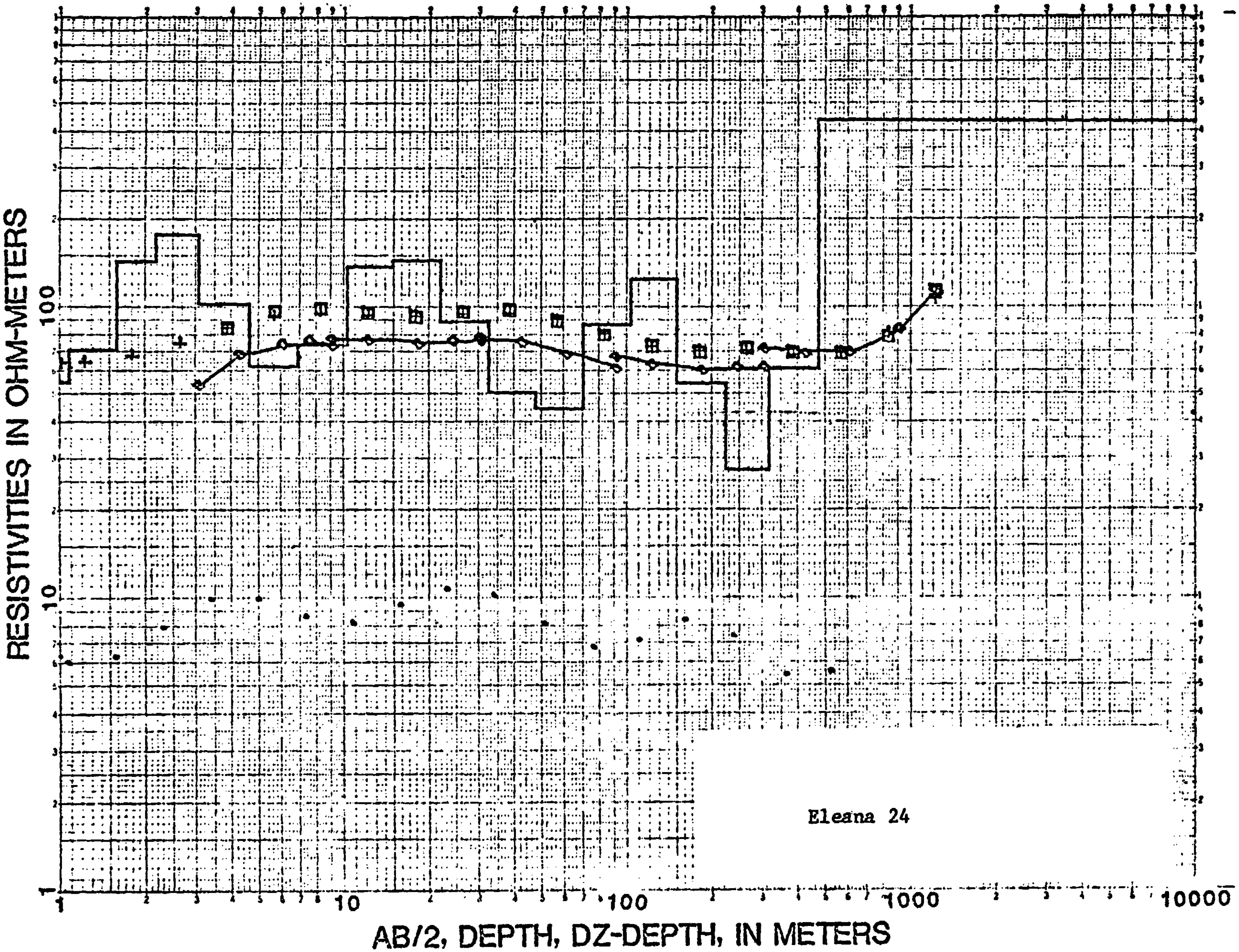
RESISTIVITIES IN OHM-METERS
100
10
1
10
100
1000
10000
AB/2, DEPTH, DZ-DEPTH, IN METERS
Eleana 24

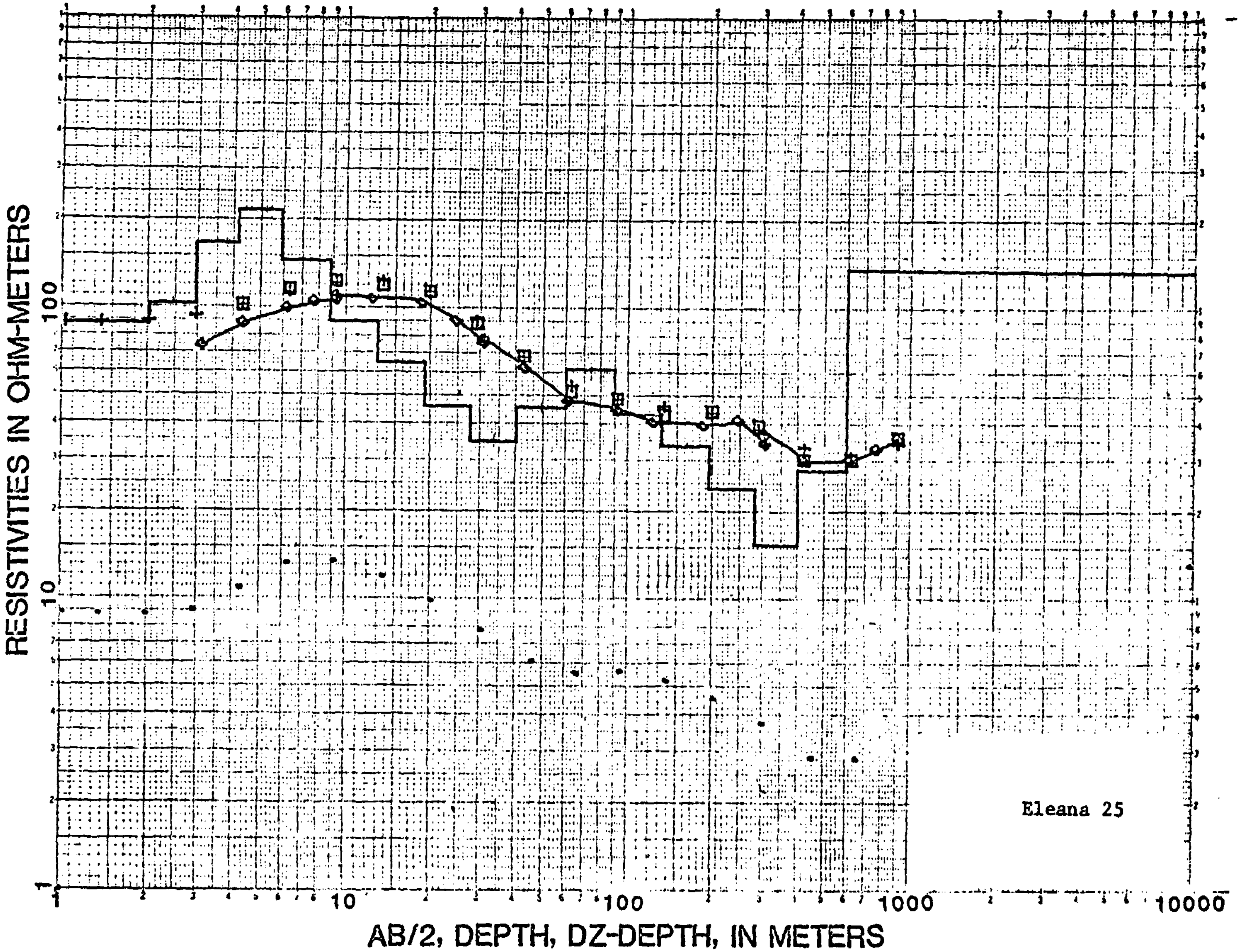
RESISTIVITIES IN OHM-METERS
100
10
1
10
100
1000
10000
AB/2, DEPTH, DZ-DEPTH, IN METERS
Eleana 25

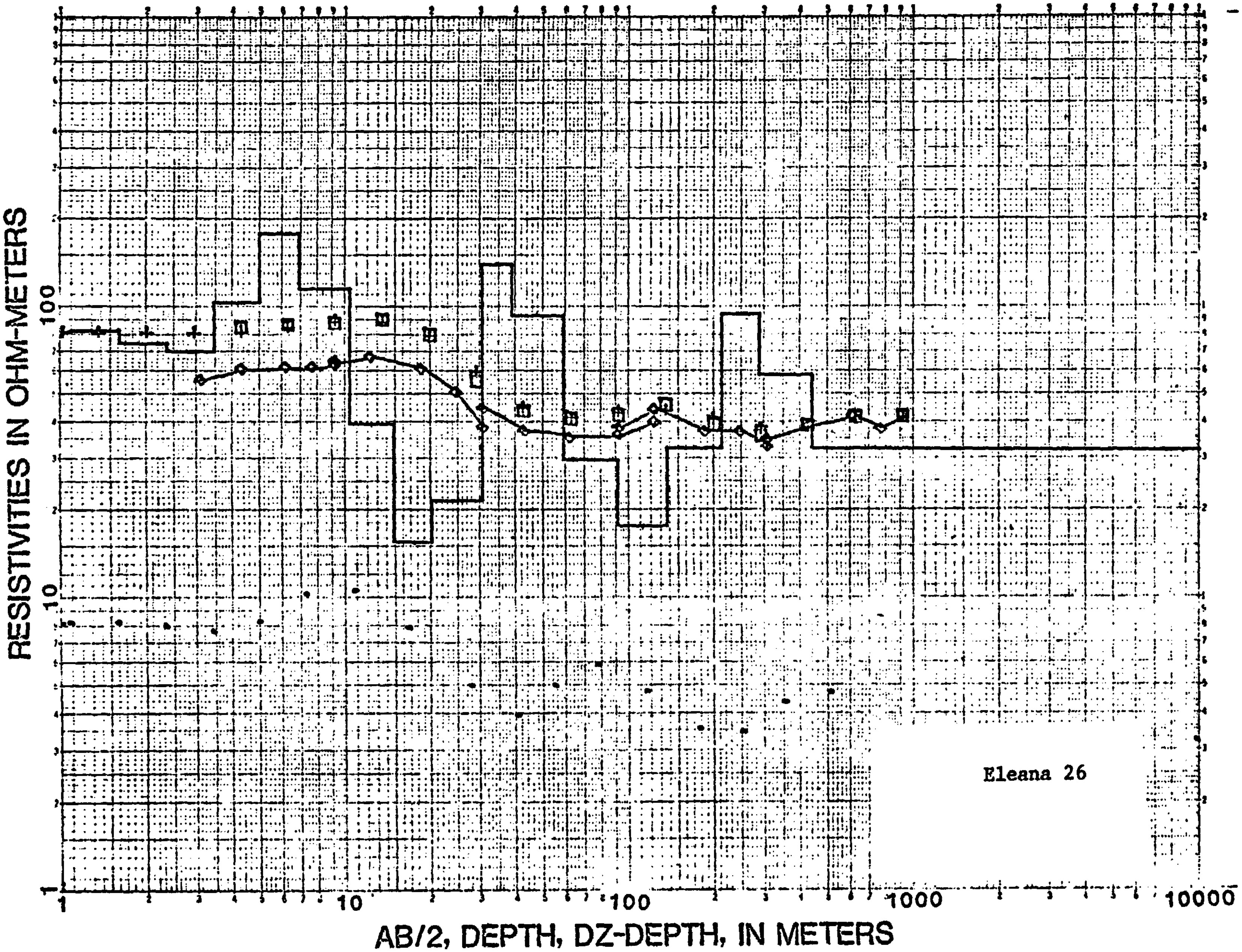
RESISTIVITIES IN OHM-METERS
100
10
1
10
100
1000
10000
AB/2, DEPTH, DZ-DEPTH, IN METERS
Eleana 26

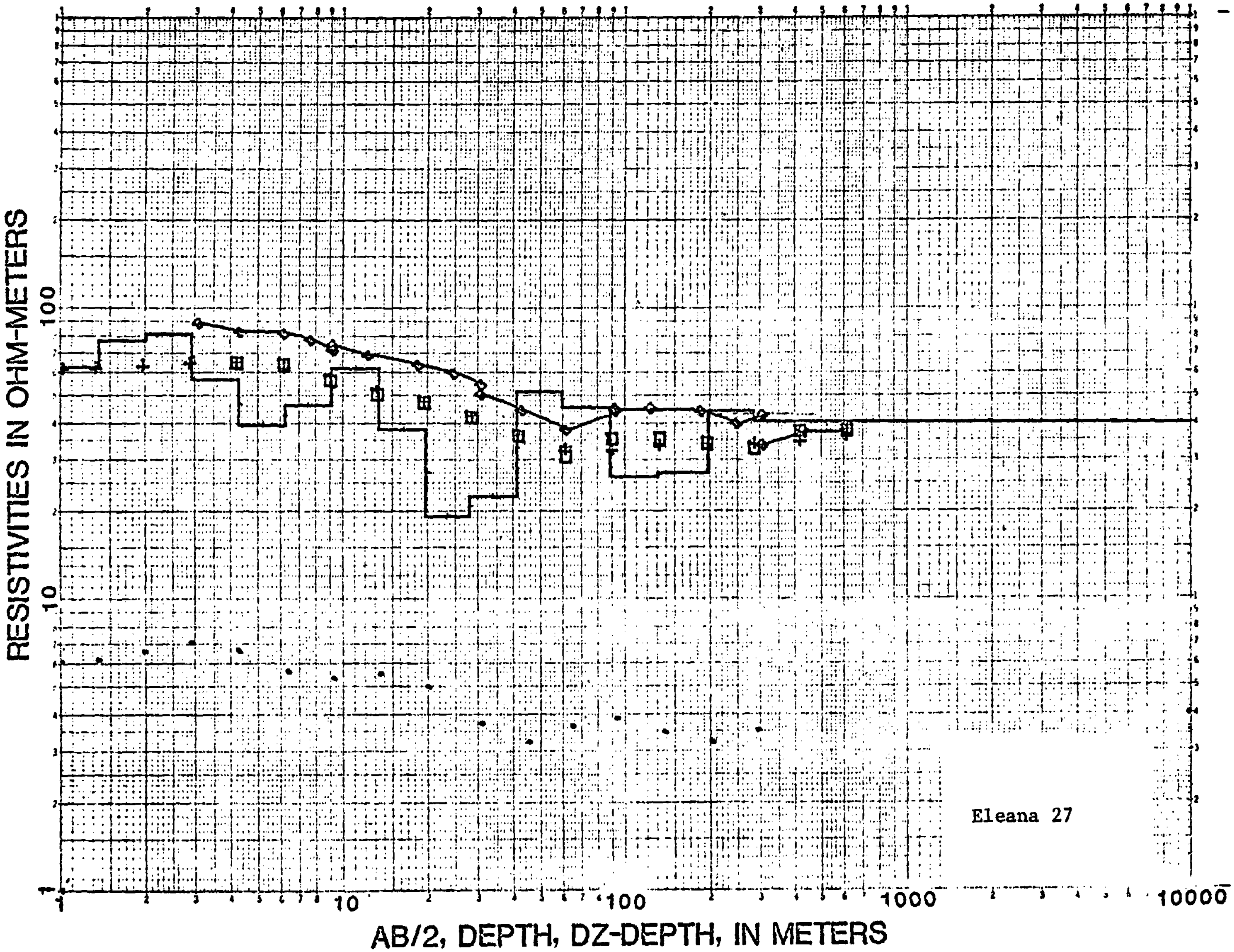
RESISTIVITIES IN OHM-METERS
100
10
1
10
100
1000
10000
AB/2, DEPTH, DZ-DEPTH, IN METERS
Eleana 27

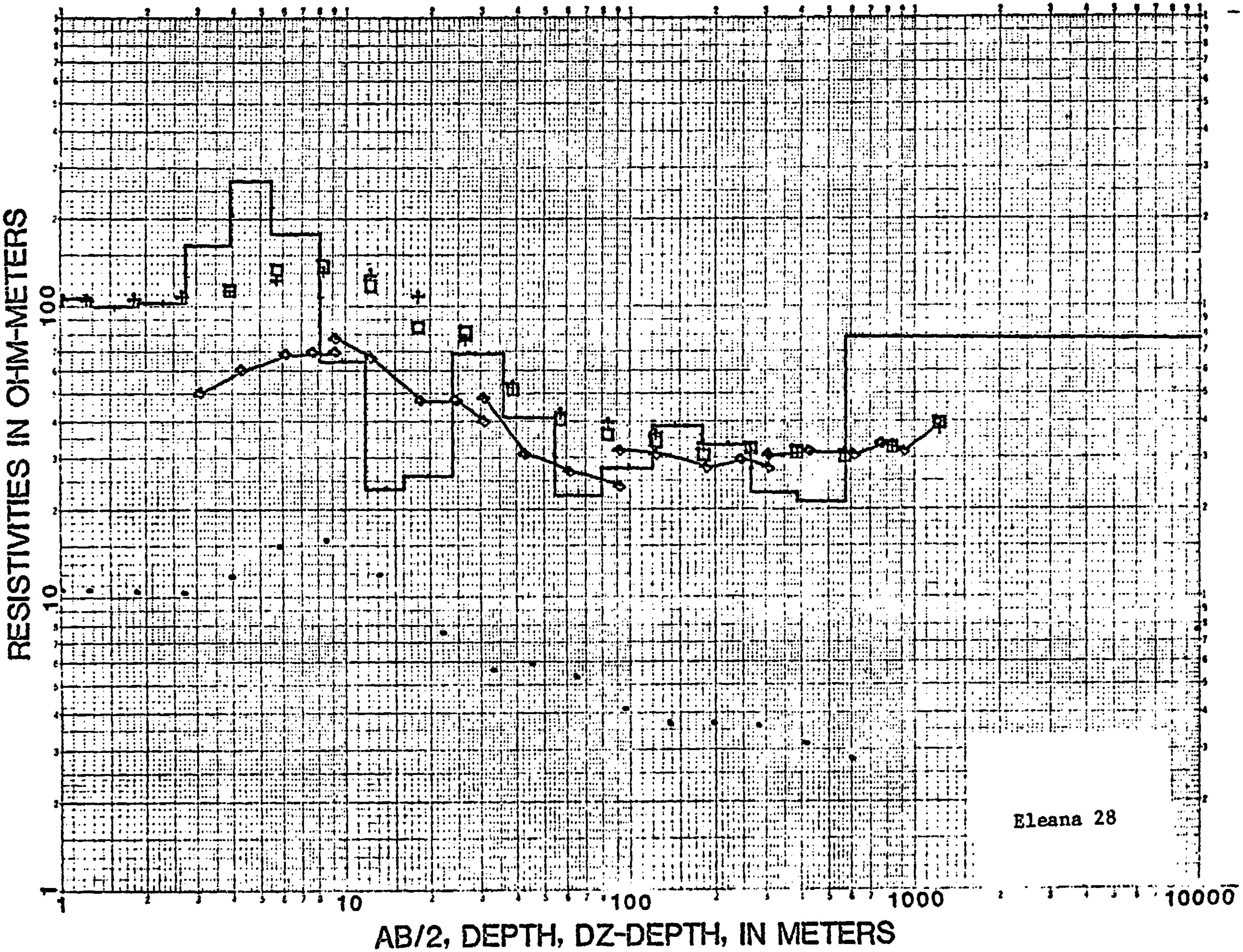

RESISTIVITIES IN OHM-METERS
100
10
1
10
100
1000
10000
AB/2, DEPTH, DZ-DEPTH, IN METERS
Eleana 28

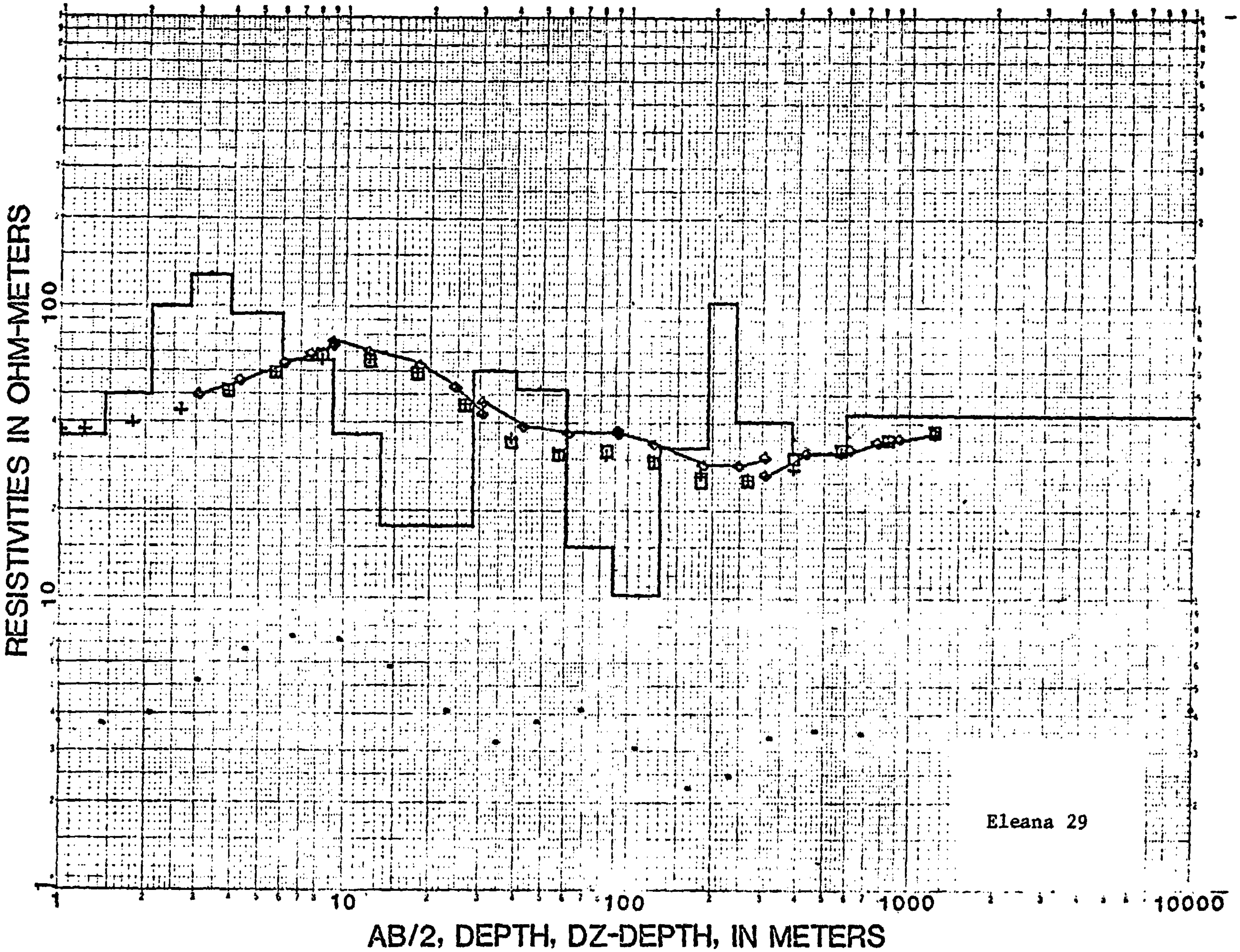
RESISTIVITIES IN OHM-METERS
100
10
1
1
10
100
1000
10000
AB/2, DEPTH, DZ-DEPTH, IN METERS
Eleana 29

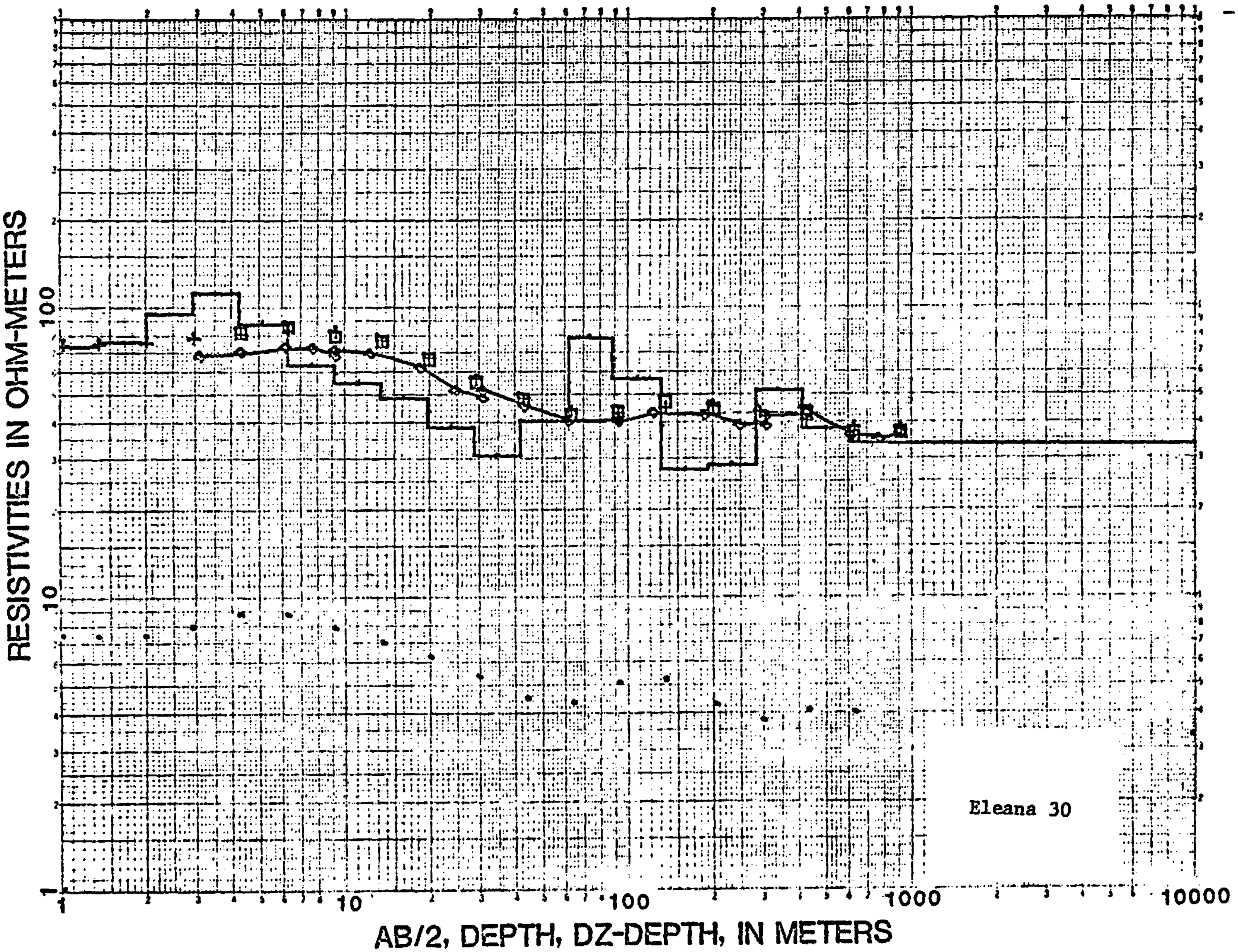
RESISTIVITIES IN OHM-METERS
100
10
1
10
100
1000
10000
AB/2, DEPTH, DZ-DEPTH, IN METERS
Eleana 30

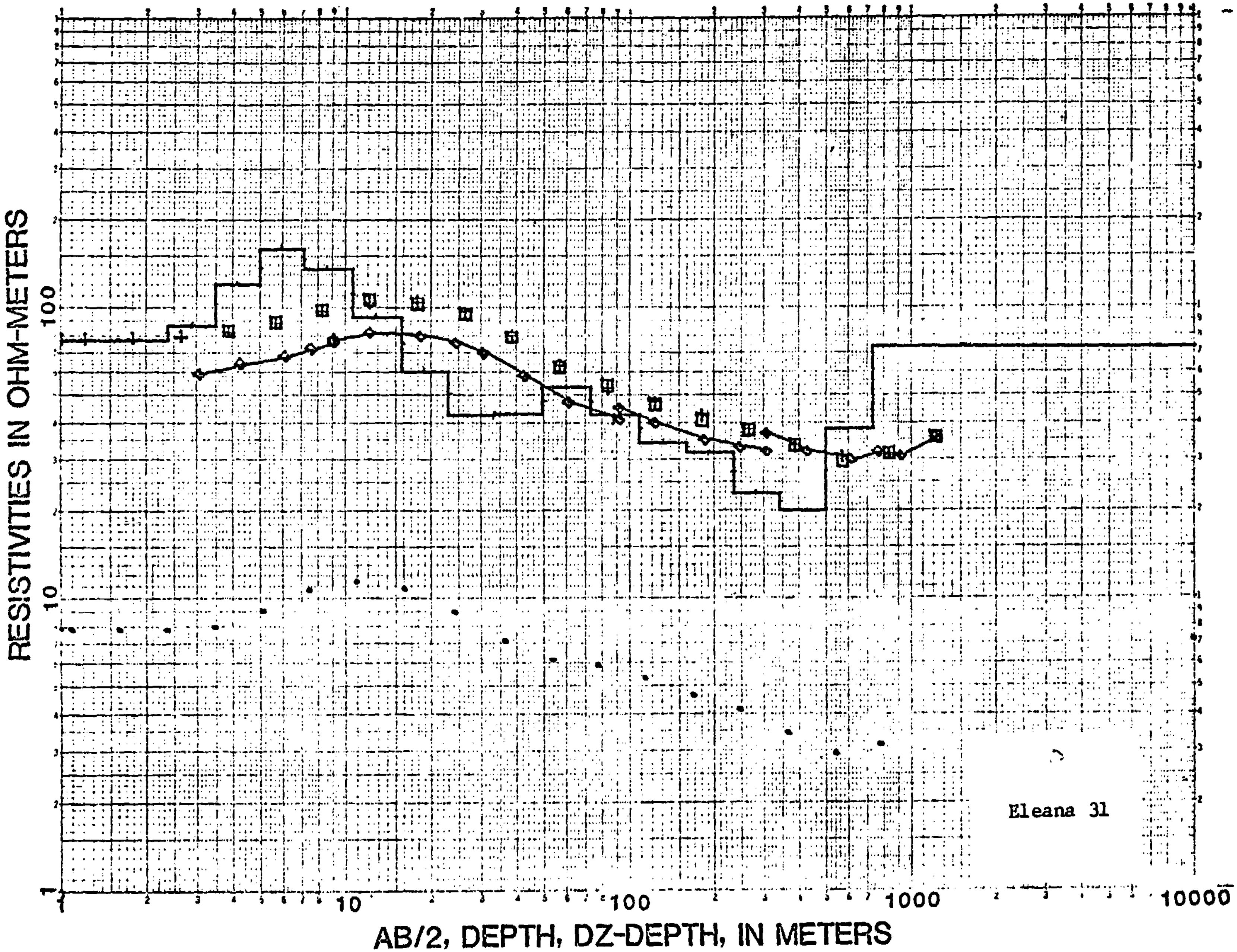
RESISTIVITIES IN OHM-METERS
100
10
1
10
100
1000
10000
AB/2, DEPTH, DZ-DEPTH, IN METERS
Eleana 31

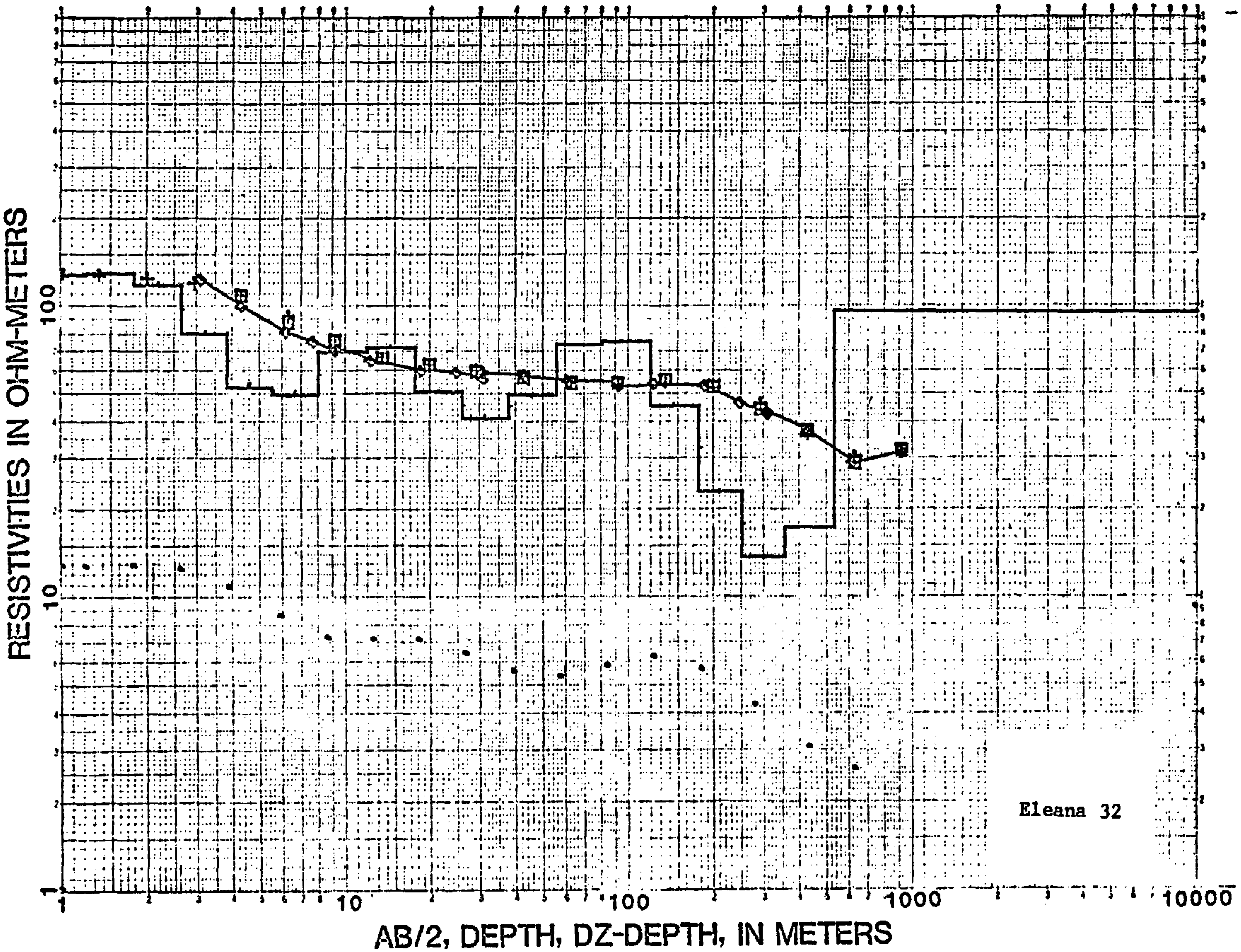
RESISTIVITIES IN OHM-METERS
100
10
1
10
100
1000
10000
AB/2, DEPTH, DZ-DEPTH, IN METERS
Eleana 32

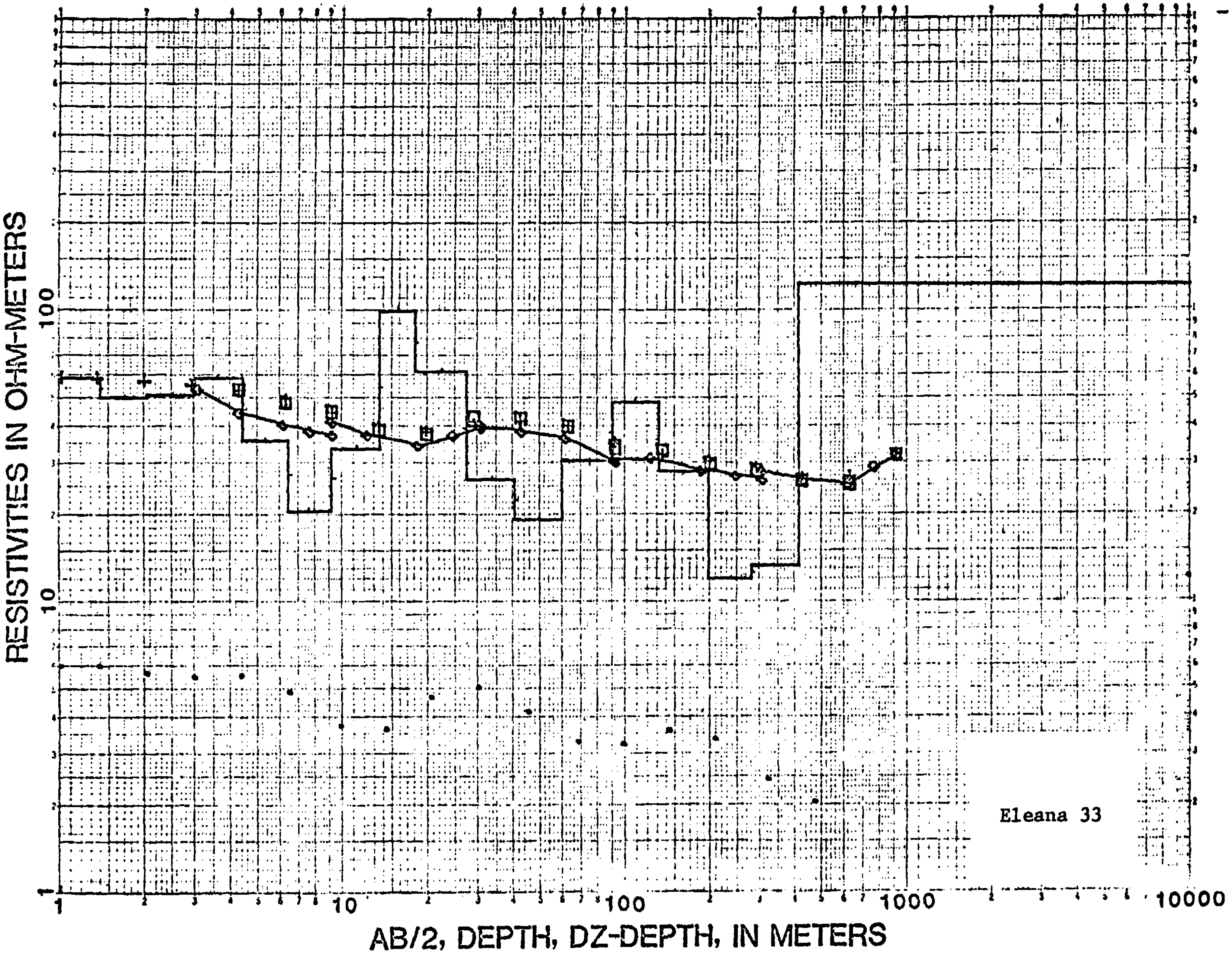

RESISTIVITIES IN OHM-METERS
100
10
1
10
100
1000
10000
AB/2, DEPTH, DZ-DEPTH, IN METERS
Eleana 33

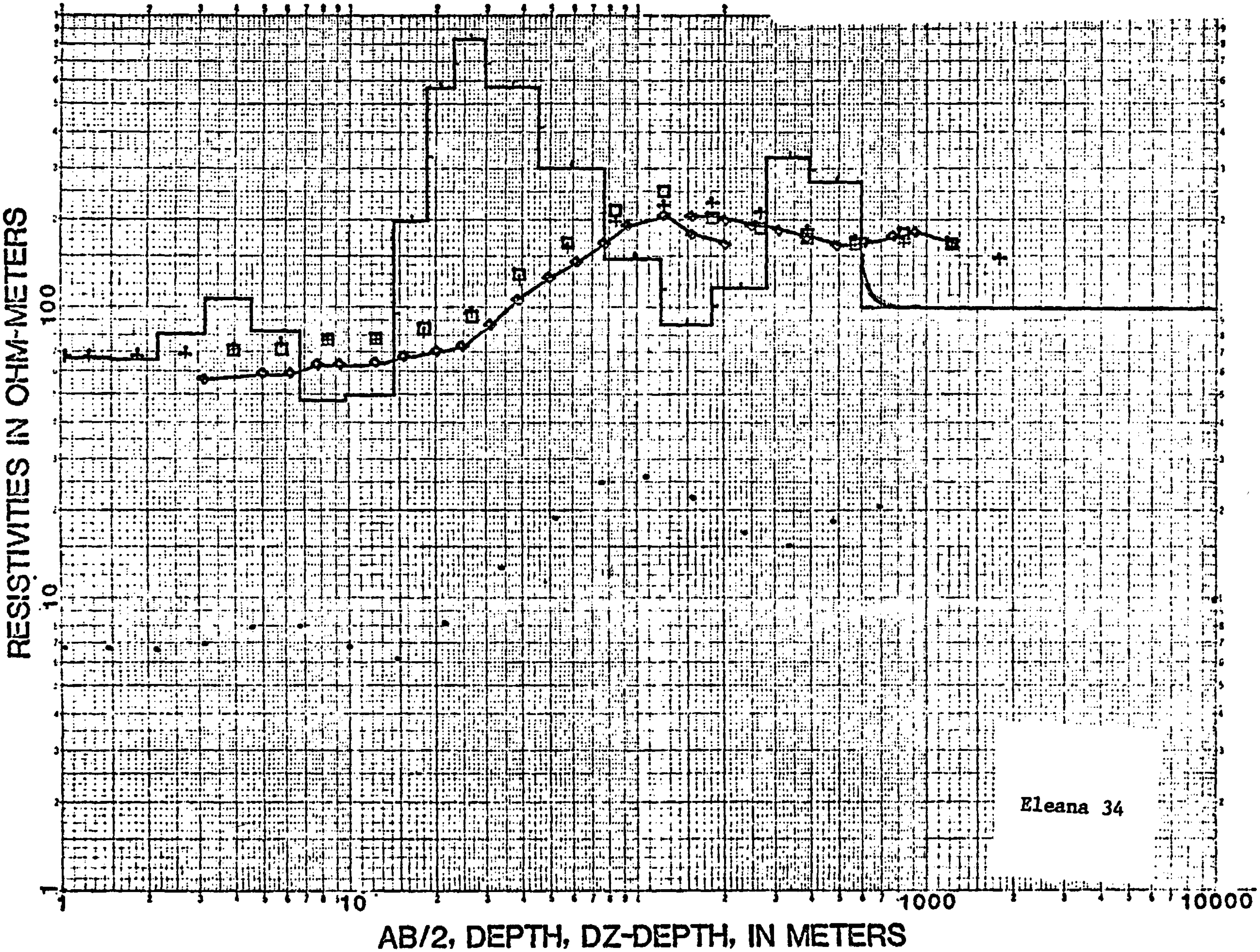

RESISTIVITIES IN OHM-METERS
100
10
1
10
1000
10000
AB/2, DEPTH, DZ-DEPTH, IN METERS
Eleana 34

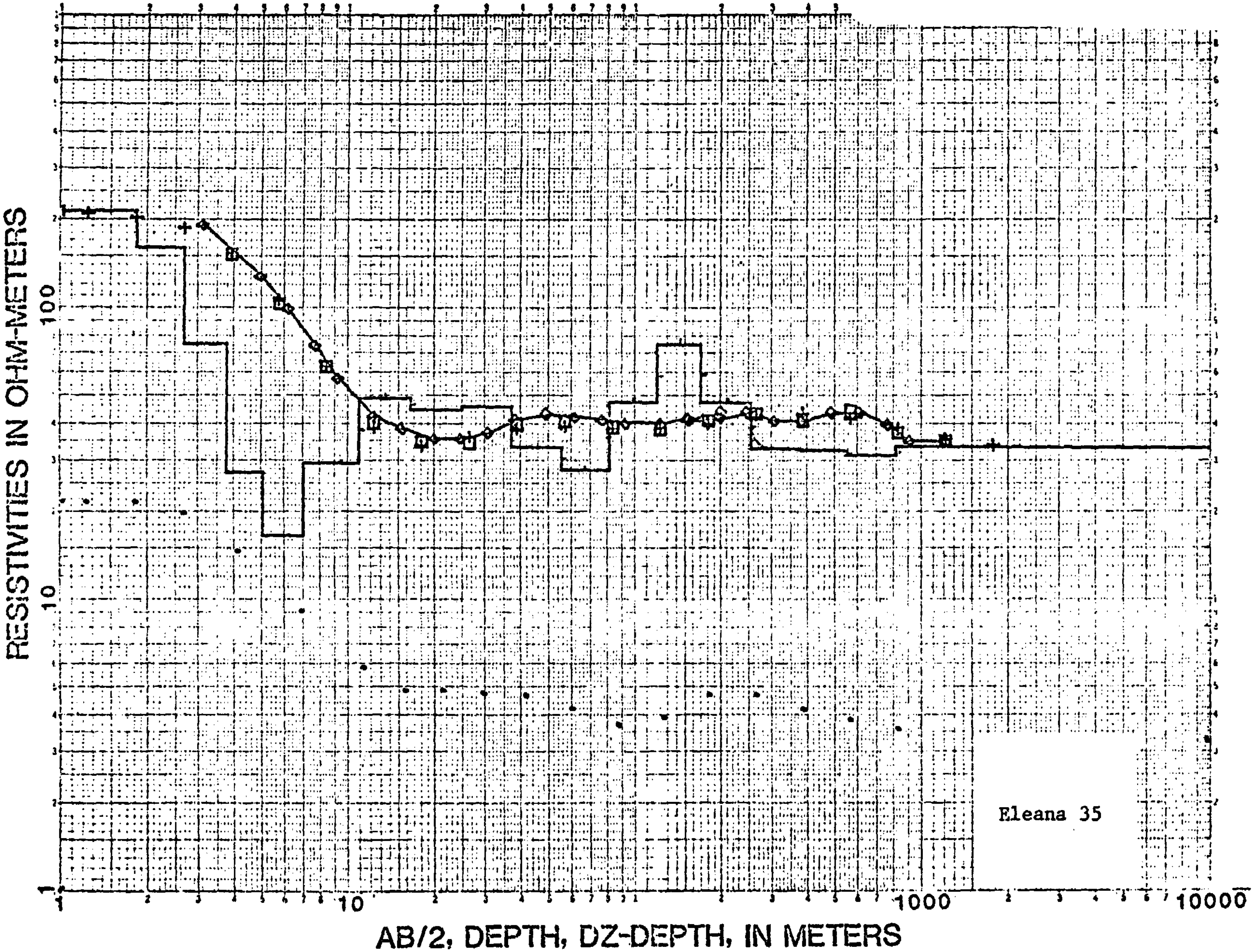
RESISTIVITIES IN OHM-METERS
100
10
1
10
1000
10000
AB/2, DEPTH, DZ-DEPTH, IN METERS
Eleana 35

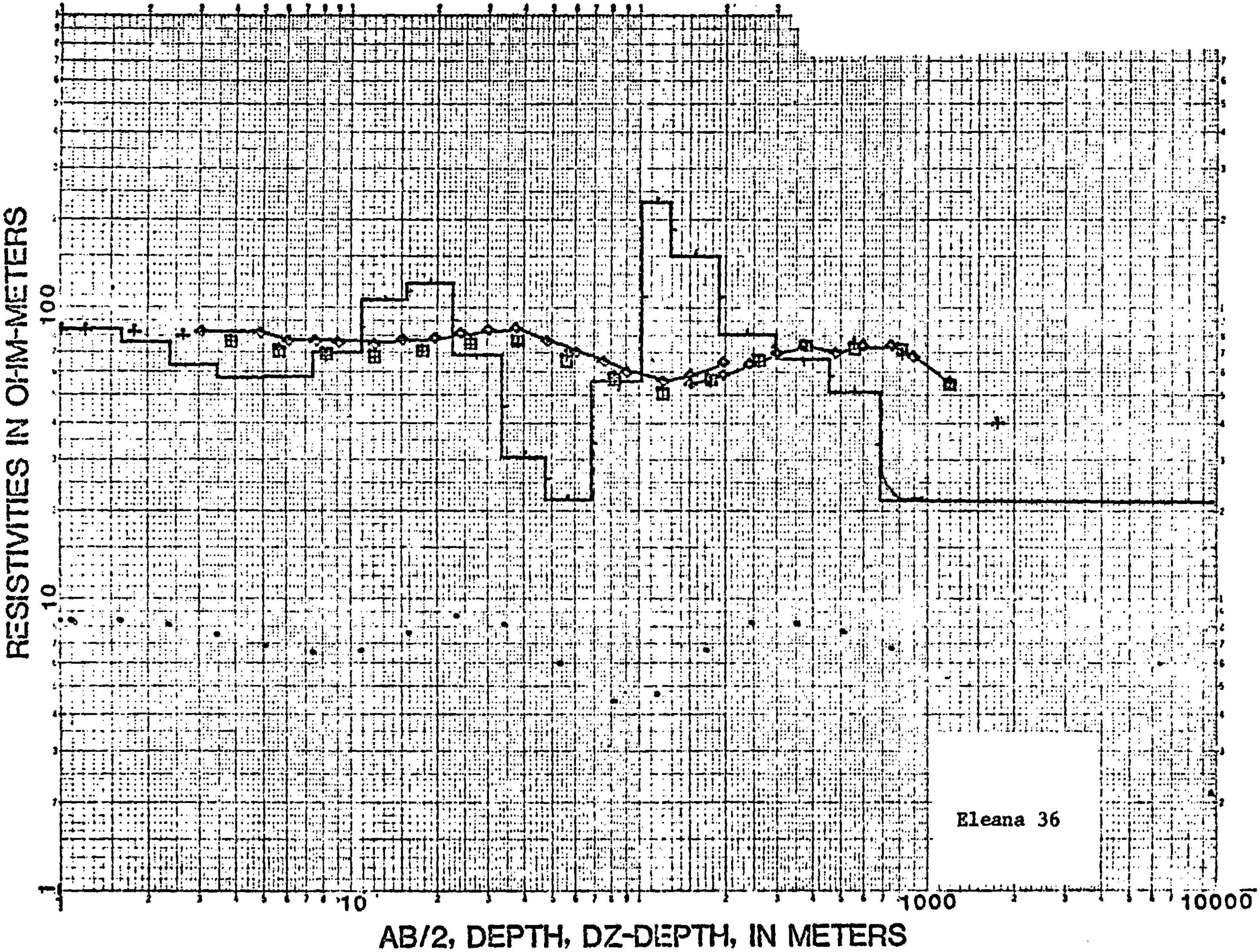

RESISTIVITIES IN OHM-METERS
100
10
1
10
1000
10000
AB/2, DEPTH, DZ-DEPTH, IN METERS
Eleana 36

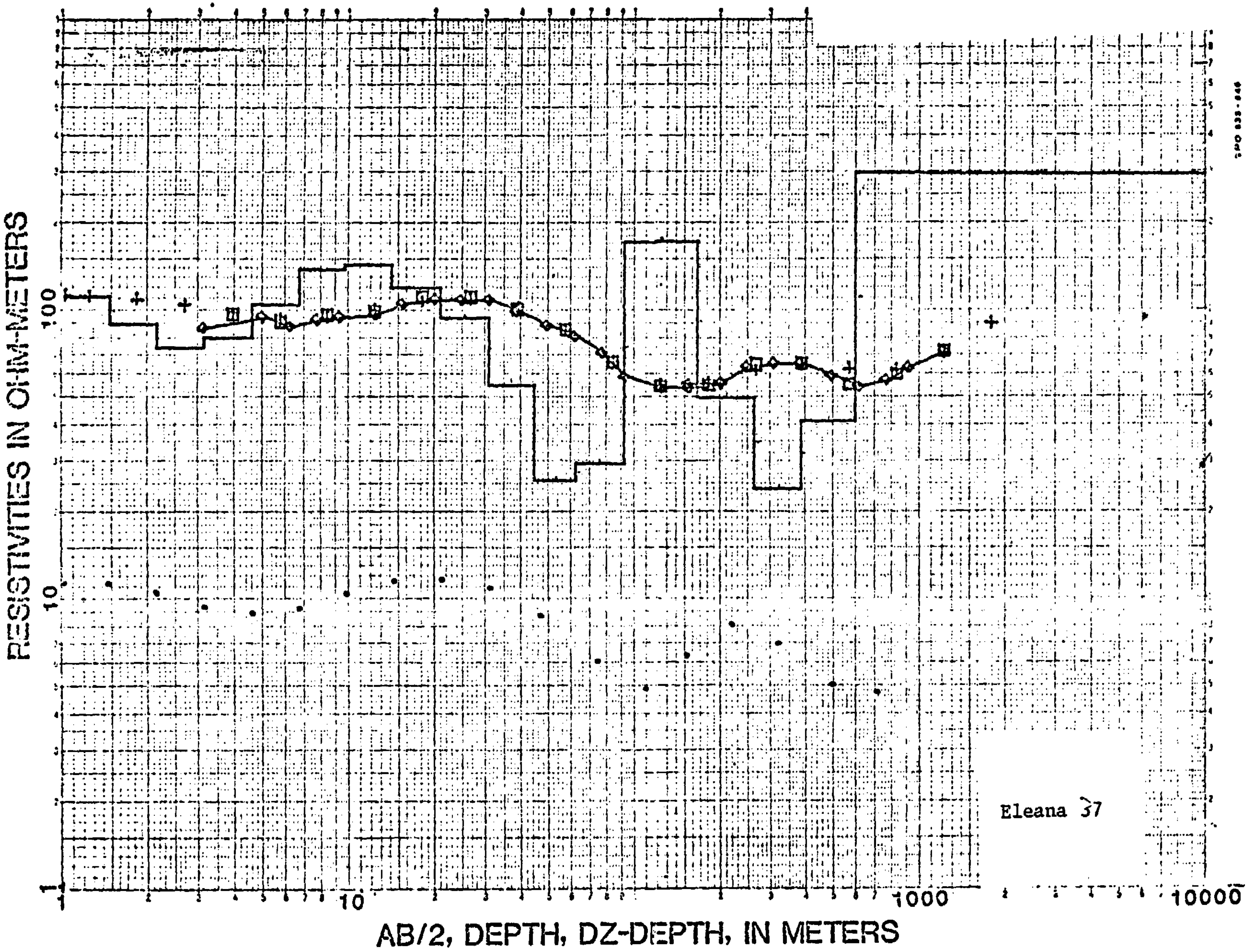
RESISTIVITIES IN OHM-METERS
100
10
1
10
1000
10000
AB/2, DEPTH, DZ-DEPTH, IN METERS
Eleana 37

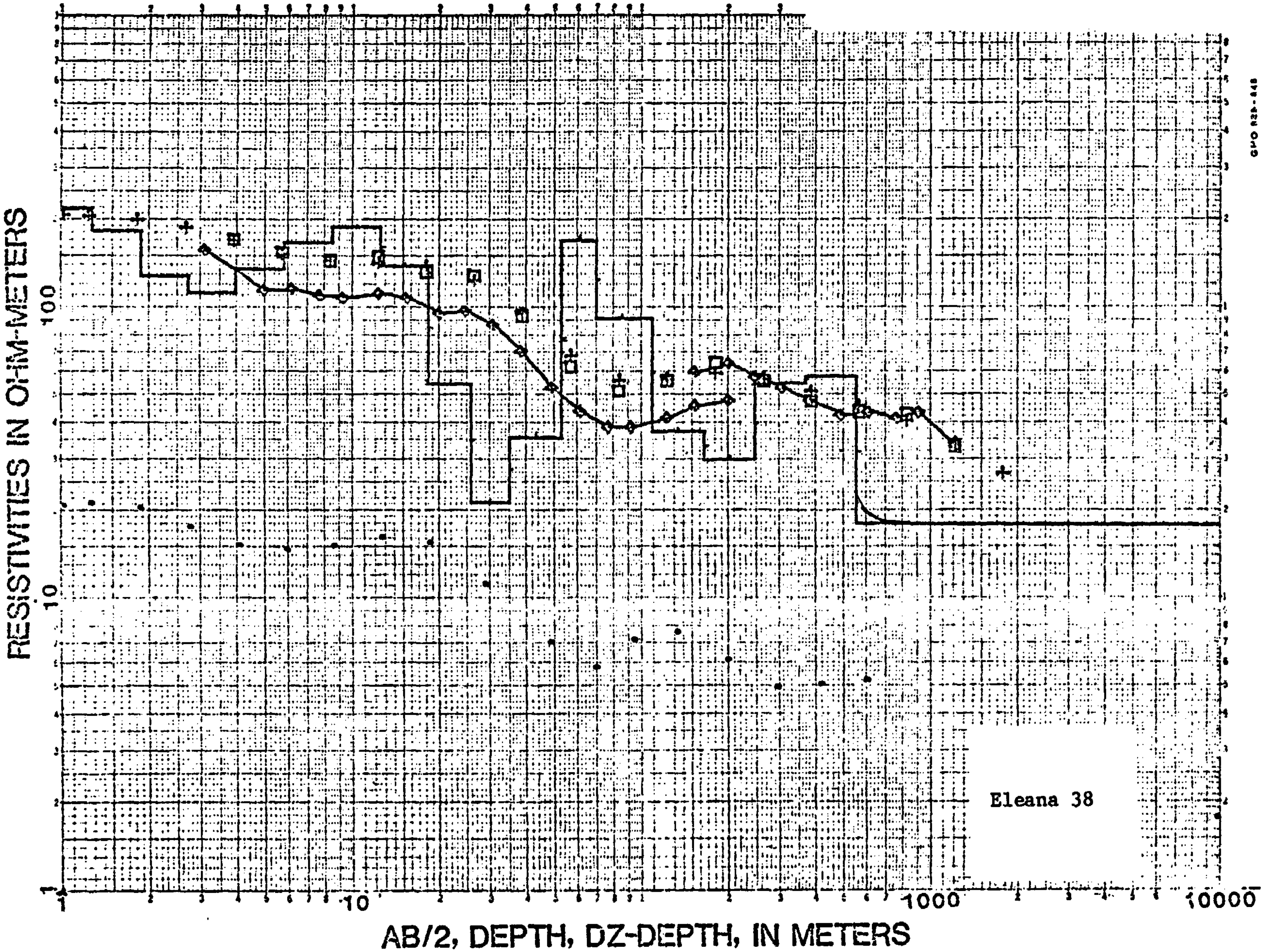

RESISTIVITIES IN OHM-METERS
100
10
10
1000
10000
AB/2, DEPTH, DZ-DEPTH, IN METERS
Eleana 38

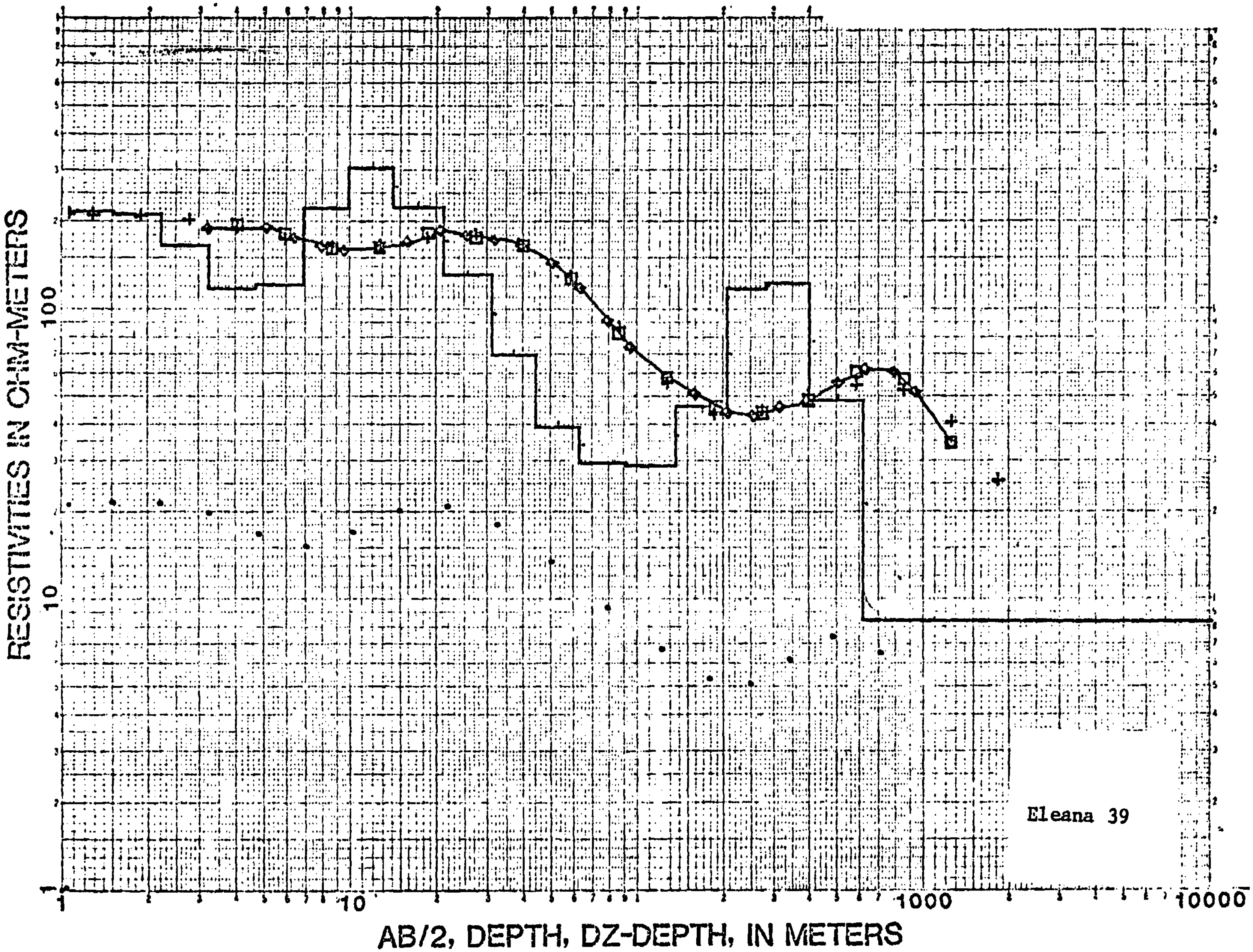

RESISTIVITIES IN OHM-METERS
100
10
1
10
1000
10000
AB/2, DEPTH, DZ-DEPTH, IN METERS
Eleana 39

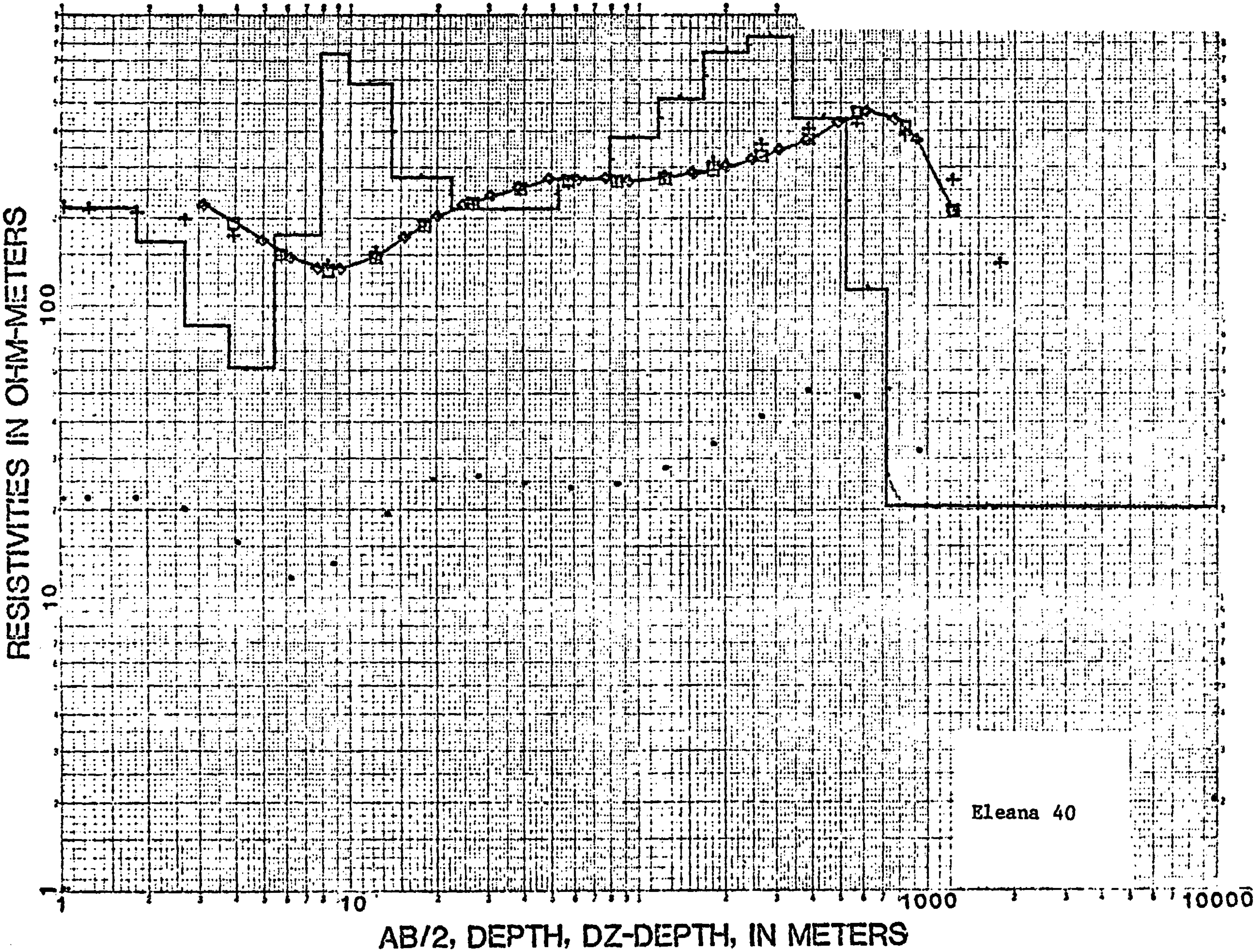
RESISTIVITIES IN OHM-METERS
AB/2, DEPTH, DZ-DEPTH, IN METERS
1
10
100
1000
10000
Eleana 40

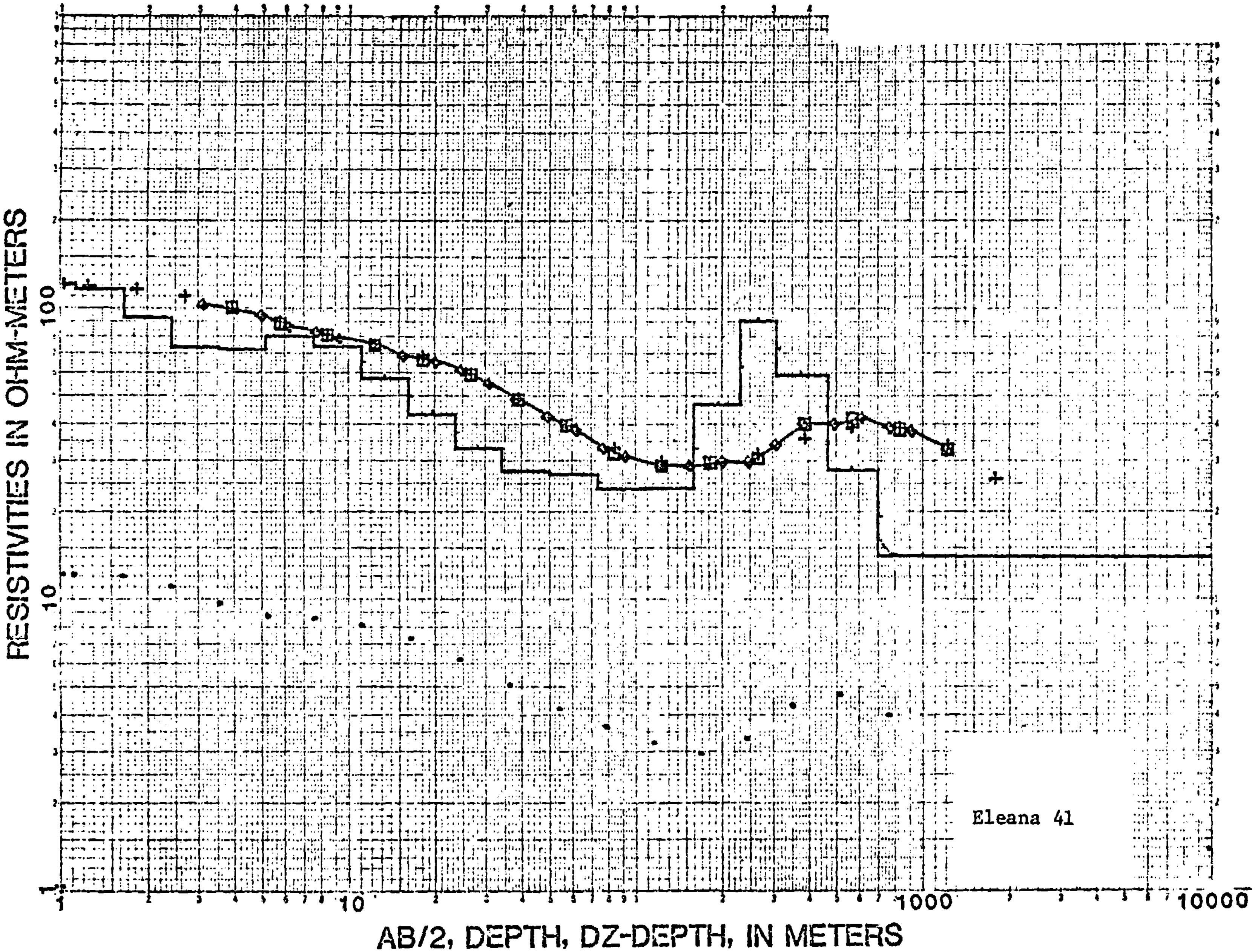

RESISTIVITIES IN OHM-METERS
100
10
1
10
1000
10000
AB/2, DEPTH, DZ-DEPTH, IN METERS
Eleana 41

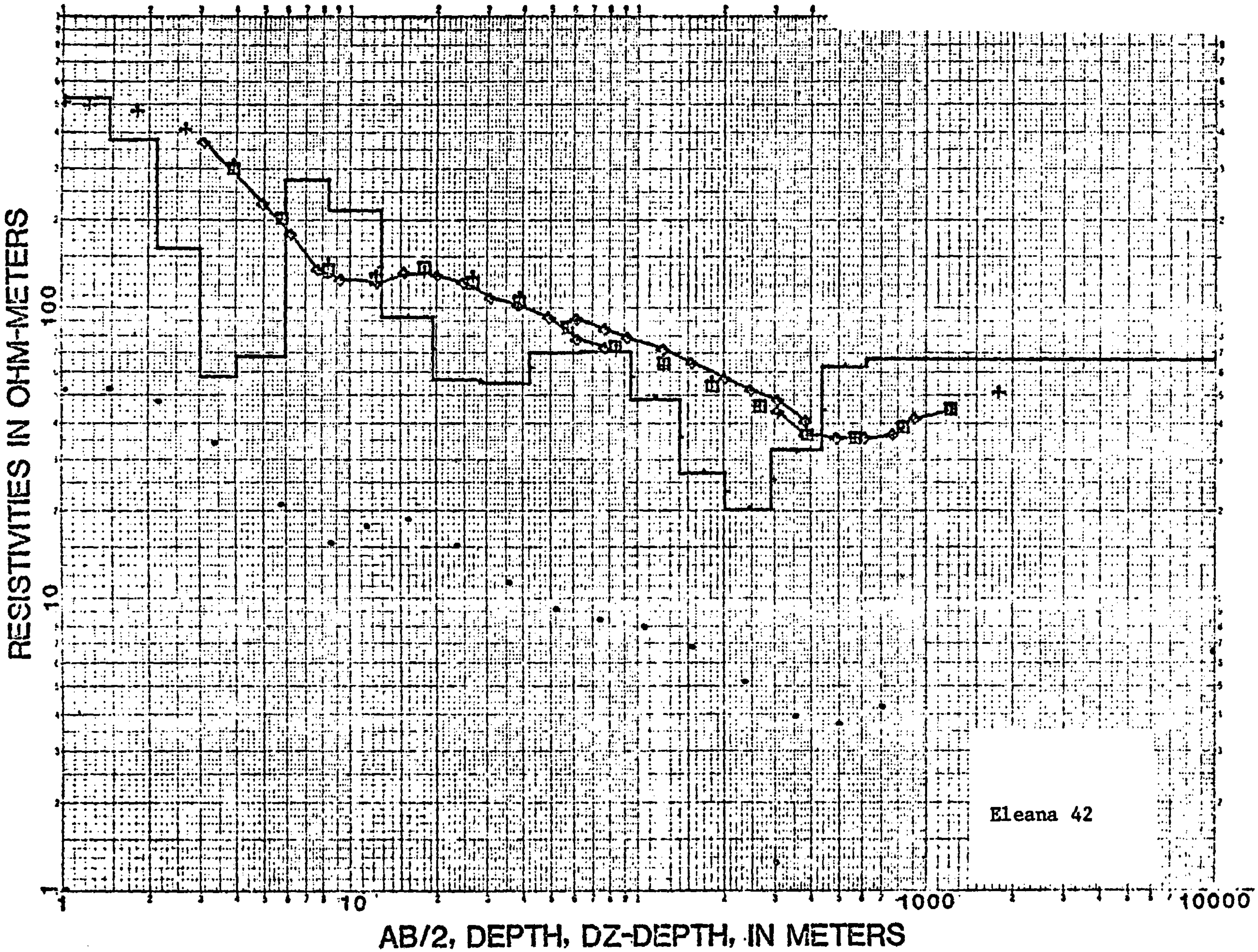
RESISTIVITIES IN OHM-METERS
AB/2, DEPTH, DZ-DEPTH, IN METERS
Eleana 42

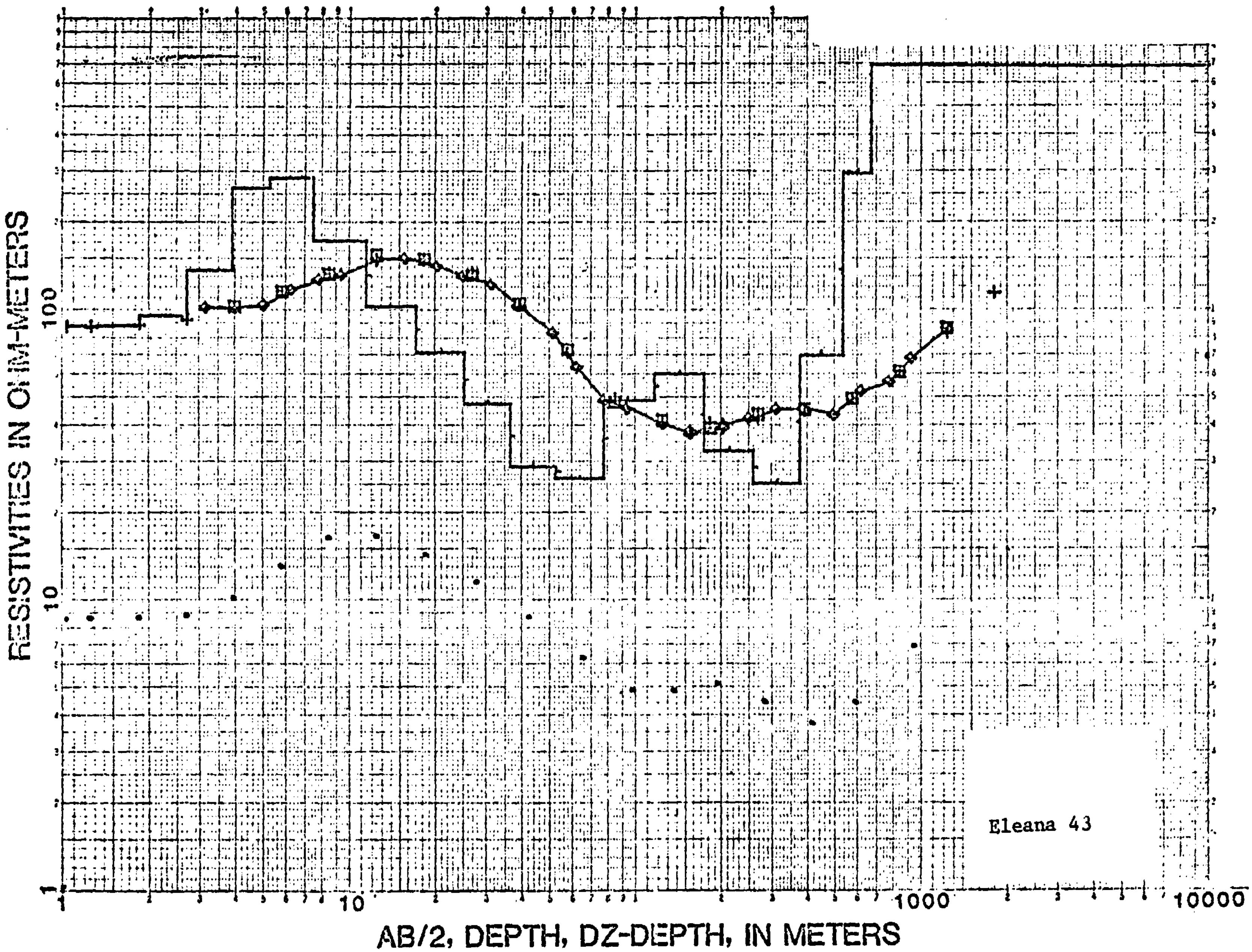
RESISTIVITIES IN OHM-METERS
100
10
1
10
1000
10000
AB/2, DEPTH, DZ-DEPTH, IN METERS
Eleana 43

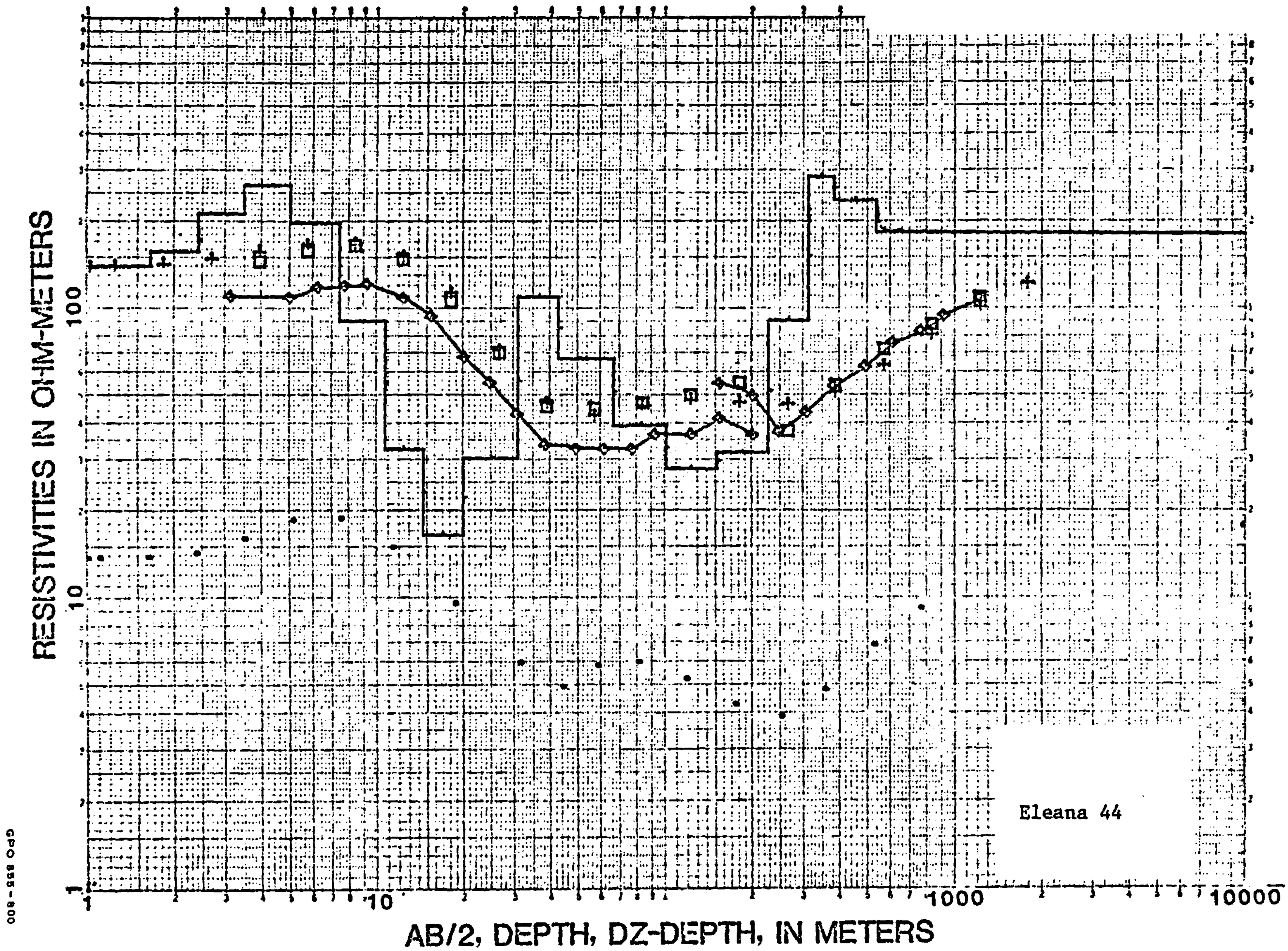
RESISTIVITIES IN OHM-METERS
100
10
1
AB/2, DEPTH, DZ-DEPTH, IN METERS
10
1000
10000
Eleana 44
GPO 885-800